Applied Catalysis B: Environment and Energy 344 (2024) 123662

Contents lists available at ScienceDirect

Applied Catalysis B: Environment and Energy

journal homepage: www.elsevier.com/locate/apcatb

Recent advances in electrocatalytic upgrading of nitric oxide and beyond

Ruping Miao [a], Dawei Chen [a,b,*], Zhiyan Guo [a], Yangyang Zhou [b,c,*], Chen Chen [b,**], Shuangyin Wang [b]

[a] College of Material Science and Engineering, Qingdao University of Science and Technology, Zhengzhou Road 53, Qingdao 266042, PR China
[b] State Key Laboratory of Chemo/Bio-Sensing and Chemometrics, College of Chemistry and Chemical Engineering, Hunan University, Changsha 410082, PR China
[c] College of Chemistry and Chemical Engineering, Jiangxi Science and Technology Normal University, Nanchang 330013, PR China

ARTICLE INFO

Keywords:
Electrocatalysis
Electrocatalyst design
Nitrogen balance
NO upgrading
C–N coupling

ABSTRACT

Turning the harmful NO into value-added chemicals is a promising alternative to achieve the electrocatalytic NO upgrading and maintain the global N-balance. However, the reaction mechanisms and electrochemical performances and are still needed to be further investigated. Herein, the development of electrochemical NO reduction and oxidation reaction (NORR and NOOR) were respectively summarized. In the NORR part, we summarized the electrocatalytic reaction systems, including directly NORR (NO to NH_3/NH_2OH) and the C-N coupling reactions with CO_x for urea, and organic molecules for amino acid, oxime. The reaction mechanisms and design principles of electrocatalysts for different reaction systems were reviewed, combining theoretical calculations and advanced characterization techniques. The NO reaction is also a potential approach to replace others cathodic reduction. Finally, the challenges and outlooks in this fields have been proposed. The electrocatalytic NO reaction not only realizes the efficient green utilization, but also provides guidance for nitrogen economy.

1. Introduction

Over the last few decades, human activities have had a significant impact on the circulation and self-balancing of the N-cycle in nature. The Haber-Bosch process is one of the greatest inventions for N_2-to-NH_3, which greatly promotes the development of agriculture but causes high concentrations nitrogen species (such as NO_3^- and NO_2^-) harmful [1]. NO is the most important component of nitrogen oxides (NO_x), which is considered as a major air pollutant mainly emitted from industrial emissions and vehicle exhaust, causing various environmental problems such as tropospheric ozone, acid rain formation, depletion of the ozone layer, and so on [2,3]. Therefore, technologies aimed at reducing NO emissions are currently the most effective and promising research direction in the pollution control field. Among the N-cycle reactions, NO is also prepared though N_2 and O_2 coupling reaction by plasma technology with the purpose of artificial nitrogen fixation for the subsequent synthesis of nitrogen compounds [4], as shown in Scheme 1. The catalytic conversion of NO is regarded as critical areas of nitrogen chemistry [5].

In recent years, several NO treatment technologies have been proposed, such as adsorption, catalytic reduction, plasma catalytic reduction, and photo/electro-catalysis [6–10]. The most common methods are selective catalytic reduction (SCR) and selective non-catalytic reduction (SNCR) techniques, where ammonia (NH_3) is used to convert nitrogen oxides into harmless nitrogen gas. [11–15]. Electrochemical NO reaction is a promising industrial alternative method to convert NO into harmless nitrogen gas, and more importantly to produce valuable chemicals with minimal carbon emissions [16]. Clearly, the electrocatalytic conversion of NO for the preparation of high value-added chemicals is more attractive.

The direct electrocatalytic reduction of nitrogen oxide can produce various products depending on the reaction conditions and catalysts, including ammonia (NH_3), NH_2OH, and so on. NH_3 is an essential chemical for human beings, playing a crucial role in the global economy [17]. A concept has been proposed to use NH_3 as a carbon-free alternative fuel, achieving zero carbon dioxide emissions [18,19]. However, the electrochemical N_2 reduction reaction (NRR) has been proposed to produce NH_3 [20,21]. The high NRR potentials are partially attributed to the scaling relationship between adsorption energies of multiple N_xH_y intermediates through the typical dissociative/associative mechanism (Scheme 2a). The adsorption energies of N-intermediates exhibit a

* Corresponding authors at: State Key Laboratory of Chemo/Bio-Sensing and Chemometrics, College of Chemistry and Chemical Engineering, Hunan University, Changsha 410082, PR China.
** Corresponding author.
E-mail addresses: daweichen@qust.edu.cn (D. Chen), zhouyangyang822@163.com (Y. Zhou), chenc@hnu.edu.cn (C. Chen).

https://doi.org/10.1016/j.apcatb.2023.123662
Received 27 September 2023; Received in revised form 19 December 2023; Accepted 22 December 2023
Available online 25 December 2023

strong linear correlation and cannot be independently optimized. Recently, the lattice nitrogen participated approach over metal nitride electrocatalysts has attracted significant attention, in which the lattice nitrogen undergoes protonation to produce NH_3 and creates nitrogen vacancies that are subsequently replenished by the reductive incorporation of N_2 (also known as the Mars-van Krevelen mechanism, Scheme 2b). However, the NRR still has the problems of low catalytic activity and low NH_3 selectivity [22].

From the thermodynamic perspective, NO has a lower bond dissociation energy (N = O, 204 kJ mol^{-1}) than N_2 (N≡N, 948 kJ mol^{-1}) and is easier to be reduced compared to NRR, thereby enhancing the reaction kinetics for NH_3 formation in aqueous phase. However, the $5e^-$ conversion process from NO to NH_3 faces significant challenges due to the HER [23]. So the important direction to improve the NH_3 conversion of NORR is to weaken the competitiveness of parallel HER and improve the electron utilization rate. The hydroxylamine (NH_2OH) is the key raw materials for the synthesis of pyridine oxime compounds, which has been wildly applied in the fields of medicine, enzyme catalysis, and sterilization. [24,25] The electrocatalytic NO reduction reaction (NORR) offers a sustainable pathway to generate NH_2OH, avoiding the high energy consumption of the traditional thermal catalytic processes [26]. Due to the presence of multiple competitive pathways and multi-electron transfer in the NORR process for NH_2OH (including hydrogen evolution reaction (HER), hydrogenation of substrate precursors, NH_3 generation, and N-N coupling), the efficient electrochemical synthesis of NH_2OH remains a big challenge.

During the NORR process, the introduction of other carbon species maybe can lead to carbon-nitrogen coupling reactions between the intermediates of carbon species and nitrogen species, resulting in the formation of new products [27]. The NO was absorbed into the catalyst surface to form adsorbed NO species (*NO), which could be coupled with *CO (from CO_2 or CO) to synthesize urea. When the *NH_2OH was formed from the hydrogenation, the abosorbed organic molecules (α-keto acids or cycloketone) on the catalyst surface could be coupled with them to synthesize amino acid, oxime, which will significantly promote the advancement of synthetic chemistry [28]. Currently, the current research is still at an early stage of development, and The reaction mechanism and reaction pathways need in-depth investigation.

In addition, the other methods for NO conversion is electrochemical NO oxidation reaction are selective catalytic reduction (SCR) and selective non-catalytic reduction (SNCR) techniques, where NO was oxidized to nitrate/nitrite (NO_2^- or NO_3^-) [29]. The more promising method for NOOR is to replace the anode reaction. The sluggish oxygen evolution reaction (OER) was the rate-determining step for cathode reduction reaction [30]. It was crucial to investigate an appropriate anodic substitution reaction with a lower overpotential for the overall energy.

In this review, we systematically re-summarized the electrocatalytic NO reactions, including the electrocatalytic NO reduction (direct NORR and C-N coupling reactions), and the oxidation reactions. The progresses in the NO reduction part were sorted out following the logic of "reductive system design" ↔ "reaction mechanism study" ↔ "electrocatalyst design" or "reaction environmental effects". With the reaction mechanism as the research direction, we focus on the catalyst structure/compositional design, including the defect engineering, crystal plane engineering, atomic engineering, coordination regulation to study the relationship between electronic structure, adsorption energy, and apparent activity sites. Finally, the current challenges and future opportunities are summarized.

2. Electrochemical NO reduction reaction

According to the annual report of China ecological environment statistics in 2021, total NO emission survey covers four types of emission sources: industrial sources, agricultural sources, domestic sources and centralized pollution treatment facilities. These four types of emission sources are subdivided into several areas, including mining, manufacturing, electricity, heat, production of gas and water, farming, livestock and poultry farming and aquaculture, the tertiary industry and household life, domestic waste disposal sites and centralized hazardous waste treatment plants. NO_x, exists in all aspects of life, has an important impact on the earth's biological and ecological environment. The development of efficient NO electrocatalytic systems, turning waste into value-added chemicals, is of great significance to the sustainable development. NO reduction generates N_2, N_2O, NH_3, and NH_2OH, the latter three of which are considered useful products [16]. Recently, electrochemical ammonia synthesis (EAS) has attracted significant attention, which can be driven by renewable energy (solar or wind power). However, the low NRR activity and NH_3 selectivity are the two major challenge [20]. The best Ru and Mo transition-metal catalysts for NRR also has much low NH_3 yield [31]. Meanwhile, the hydrogen evolution reaction (HER) as the competing reaction is more preferred than NRR, leading to much low Faradaic efficiencies (FE) of NH_3. This section discusses recent methods of improving the NORR active and selective, including the theoretical calculation and the regulation of mass transfer, solution environment, and the structural properties of

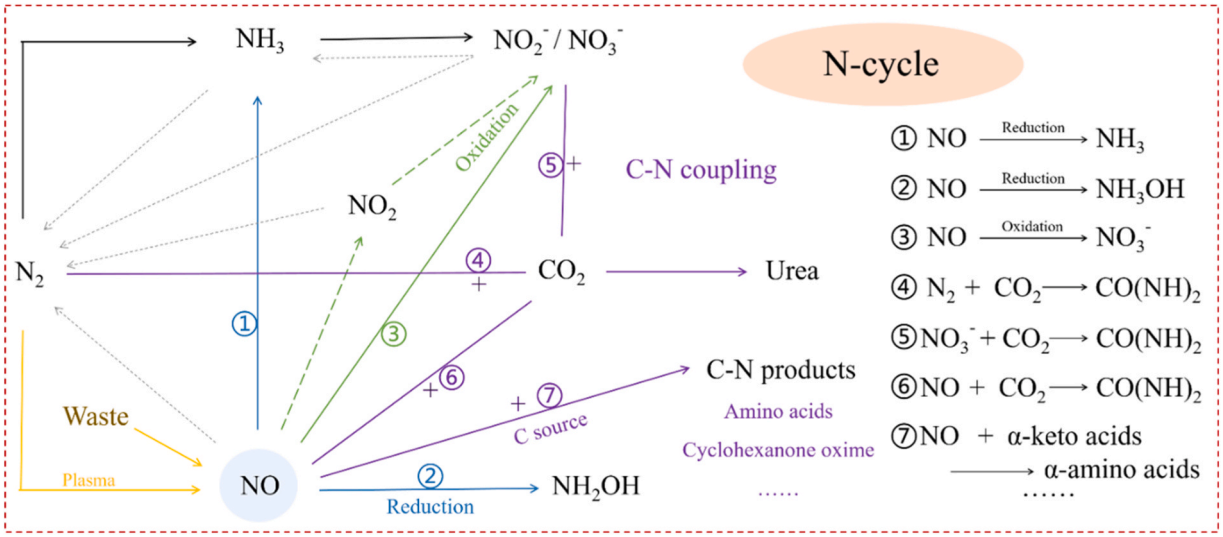

Scheme 1. Main pathways of NO in N-cycle and the reduction, oxidation, and C-N coupling reactions.

catalysts (defect, crystal plane, coordination, atoms engineering, and so on).

2.1. Reaction mechanisms of NORR

2.1.1. Potential regulation

The applied potential is a critical factor to regulate the product selectivity in NORR, and there are different products depending on potential [32]: $2NO + 4(H^+ + e^-) \rightarrow N_2 + 2\ H_2O$, $E_0 = 1.68$ V; $2NO + 2(H^+ + e^-) \rightarrow N_2O + 2\ H_2O$, $E_0 = 1.59$ V; $NO + 5(H^+ + e^-) \rightarrow NH_3 + H_2O$, $E_0 = 0.71$ V; $NO + 3(H^+ + e^-) \rightarrow NH_2OH$, $E_0 = 0.38$ V. Obviously, it was found that N_2 and N_2O is the main product at high (positive) potentials, and NH_3 and NH_2OH will be dominant at relatively low (negative) potentials. In addition, when potential goes below 0 V vs. RHE, the competitive hydrogen evolution reaction (HER) becomes pronounced: $2(H^+ + e^-) \rightarrow H_2$, $E_0 = 0$ V. The NRR activity is always lower than HER for all the transition metals, resulting in low NH_3 selectivity. However, the NH_3 production is more preferred than HER by about 0.65 V in limiting potential for the NORR scenario (Fig. 1a). The limiting steps for N_2 and N_2O formation are N-N and N-NO coupling, with the barriers of 0.92 and 0.60 eV, respectively. The highest barrier to reduce N * to NH_3 is 0.50 eV, which is lower than the N-NO and N-N coupling (Fig. 1b).

A micro-kinetic model to rationalize the general selectivity trend of NORR by Ag catalyst with varying potential was studied [33]. It showed the selectivity turnover from N_2O to NH_3 and from NH_3 to H_2 involves two key factors. The first turnover is influenced by the thermochemical coupling of two NO* species, which limits the production of N_2O. The second turnover is attributed to the larger transfer coefficient of the hydrogen evolution reaction (HER) compared to that of NH_3. The electrode potential could change the NORR selectivity.

2.1.2. Catalytic route regulation

In a typical NORR process, the status of the N-O bond (maintenance or breaking) plays a crucial role in regulating product selectivity [34]. Notably, the bonding energy of the N-O bond can be modulated by the adsorption configuration on catalyst surfaces [35], which can be controlled by adjusting the atomic structure of the catalysts [36,37]. The investigations on reaction mechanisms mostly rely on the density functional theory (DFT) calculations and in-situ characterizations. Understanding the mechanisms of NORR holds the key to the electrocatalyst design with high selectivity for high value-added NH_3 or NH_2OH. Accordingly, two representative reaction mechanisms (NO to NH_3, and NO to NH_2OH) will be introduced and discussed in this section.

2.1.2.1. NO to NH_3. The NRR activity is consistently lower than HER, but for Cu (111), NH_3 production is favored over HER by approximately 0.65 V at in the NORR scenario (Fig. 1a). The Cu atoms can bind with *NO more well than *H, showing a higher selective and activity for NH_3 formation than other transition metals [38]. Through thermodynamic estimation, Cu has also been identified as the most active catalyst (among V, Cr, Mo, Pd, Ru, Rh, Pt, Ag, et al.) for the conversion of NO to NH_3 [39]. Generally, the possible NORR products include H_2, NH_3, N_2O, and N_2. Fig. 1b shows that the highest barrier for the continuous reduction of N * to NH_3 is 0.50 eV, which is lower than that of N * to N_2O or N_2. The desigh strategy of screening single-atom catalysts (SACs) for NO-to-NH_3 reachtion via systematic first-principles calculations was reported. Among the TM-C_2N (TM= Ti, V, Cr, Mn, Zr, and Hf), the SACs Zr-C_2N is selected as a stable NO-adsorbable for NORR with high NH_3 selectivity. The possible mechanisms of NO-to-NH_3 includes O-distal, O-alternating, N-distal, and N-alternating pathways, and it is worth noting that all pathways start with the N-end pattern of NO and involve the N-O bond breaking (Fig. 1c).

2.1.2.2. NO to NH_2OH. Co single-atom catalysts (SACs) are designed to regulate the adsorption configuration of NO, resulting in the desired product (NH_2OH) generation (Fig. 1d) [40]. For Co SACs, linear adsorption (vertical and bent adsorption) of NO on isolated Co sites maintains the N-O bonds during the reaction process, leading to the selective production of NH_2OH via intermediates such as *HNO and $*H_2NO$. In addition, Co nanoparticles (Co NPs) are synthesized to control the adsorption configuration of NO for selective reduction, and the bridging adsorption of NO on adjacent Co sites facilitates the breaking of the N-O bond, promoting NH_3 formation through dissociation (Fig. 1d). It demonstrates that Co SACs exhibit a high NH_2OH selectivity (FE_{NH2OH}: 81.3%), but Co NPs display high NH_3 selectivity (FE_{NH3}: 92.3%). To investigate the source of these small amounts of NH_3, formaldehyde was added to the NO reduction process to capture the generated NH_2OH in situ (Fig. 2a, d). Attenuated total reflectance (ATR) infrared spectrum testing technology can obtain the absorption spectrum, the chemical composition and structure information of the surface layer of the sample. Through a combination of in situ electrochemical attenuated total reflection Fourier transform infrared (ATR-IR) spectroscopy, online

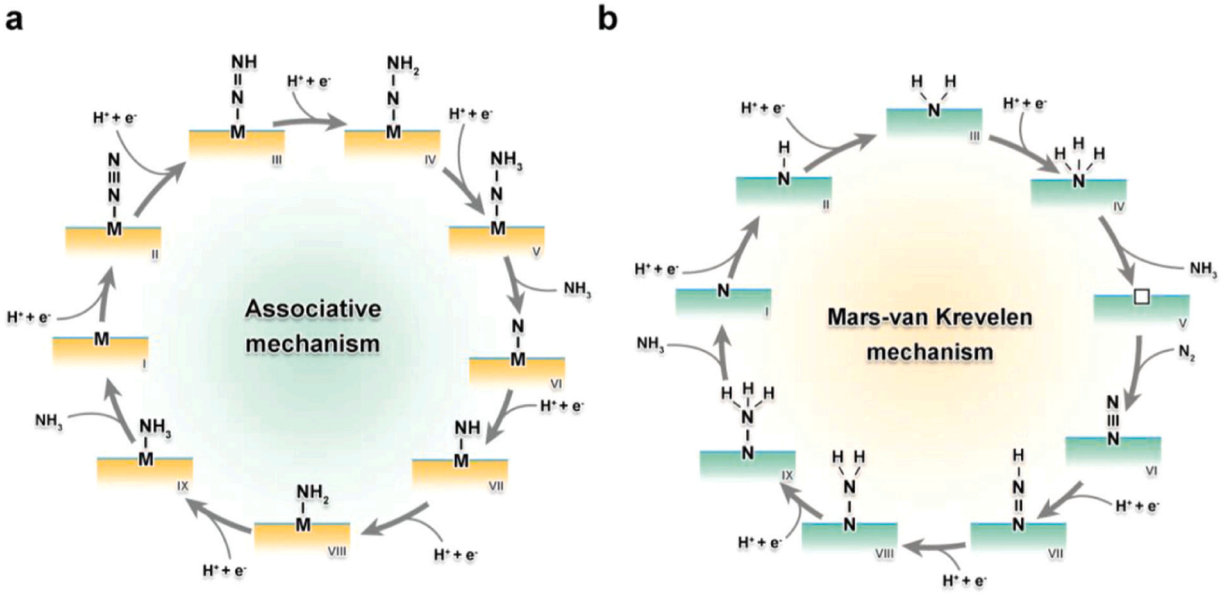

Scheme 2. The electrocatalytic NRR mechanisms. a) The dissociative mechanism. b) The Mars-van Krevelen mechanism. Copyright 2023, Wiley-VCH.

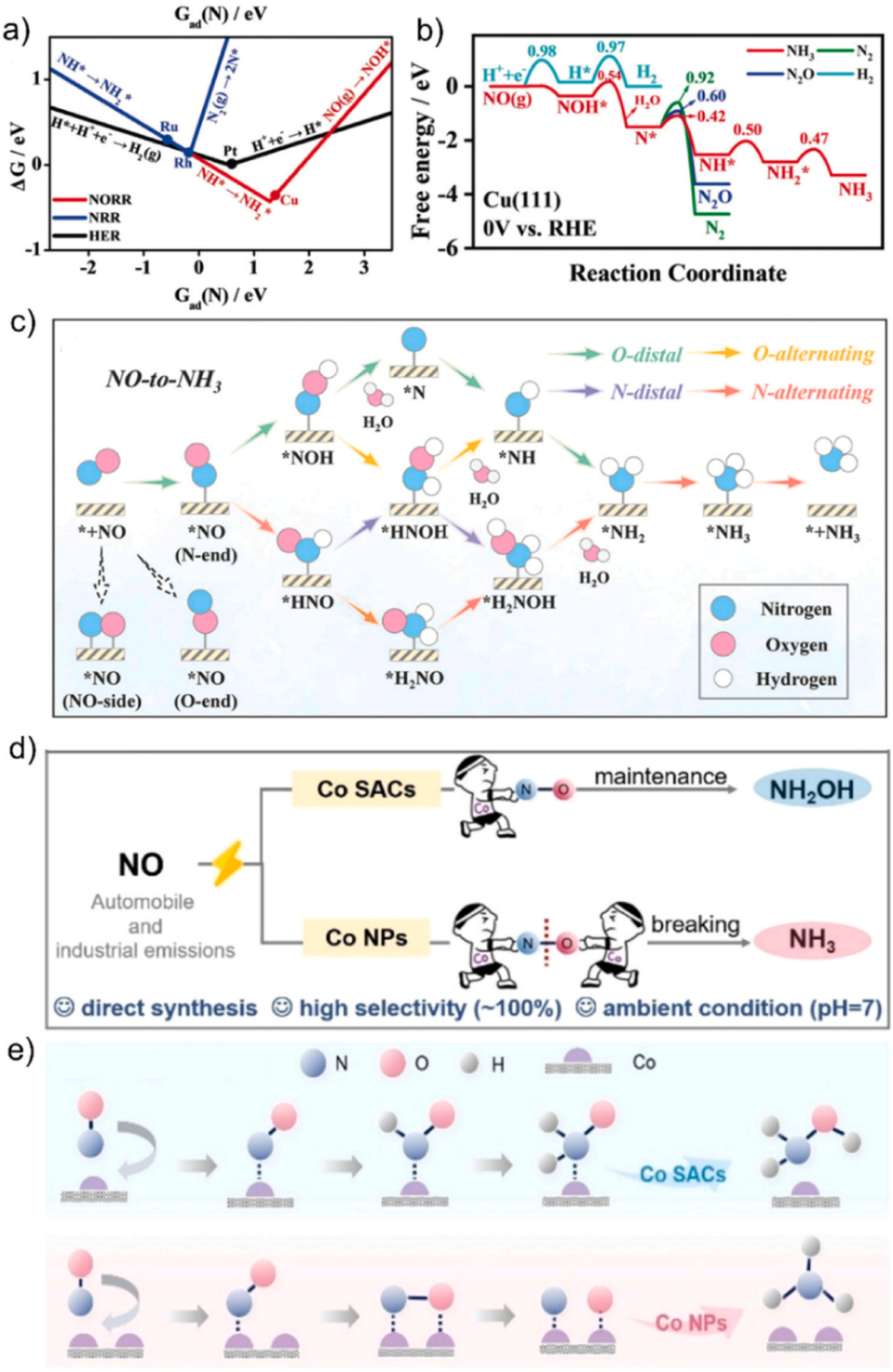

Fig. 1. a) Comparison of the ΔG-determining steps between NORR, NRR, and HER. b)Free-energy diagrams for HER, NORR to NH_3, N_2O, and N_2. c) Schematic illustration of NO-to-NH_3. d) Schematic diagram for the catalysts design for NO selective reduction. e) Deduced NORR pathway on Co SACs and Co NPs for NH_2OH and NH_3, respectively. Copyright 2023, Wiley-VCH.

differential electrochemical mass spectrometry (DEMS) tests, and theoretical simulations, the mechanism behind the regulation of product selectivity was revealed. Notably, the free energy of $*NH_2O \rightarrow * + NH_2OH$ (−0.46 eV) was lower than that of $*NH_2O \rightarrow * + NH_3$ (−0.22 eV) (Fig. 5f), leading to the selective production of NH_2OH. By controlling the adsorption configuration, the selective reduction of NO can be effectively achieved, guiding the advanced catalyst design.

2.2. The design principle for NORR catalysts

Significantly, the activation of NO molecules is comparatively easier than that of N_2 owing to its lower dissociation energy. It is worth mentioning that the standard reduction potential of NORR (0.71 V vs RHE) is more positive than that of NRR and HER, suggesting that NORR is thermodynamically more favorable than NRR (Fig. 3a). Exploring efficient electrocatalysts for high NORR performance continues to pose a

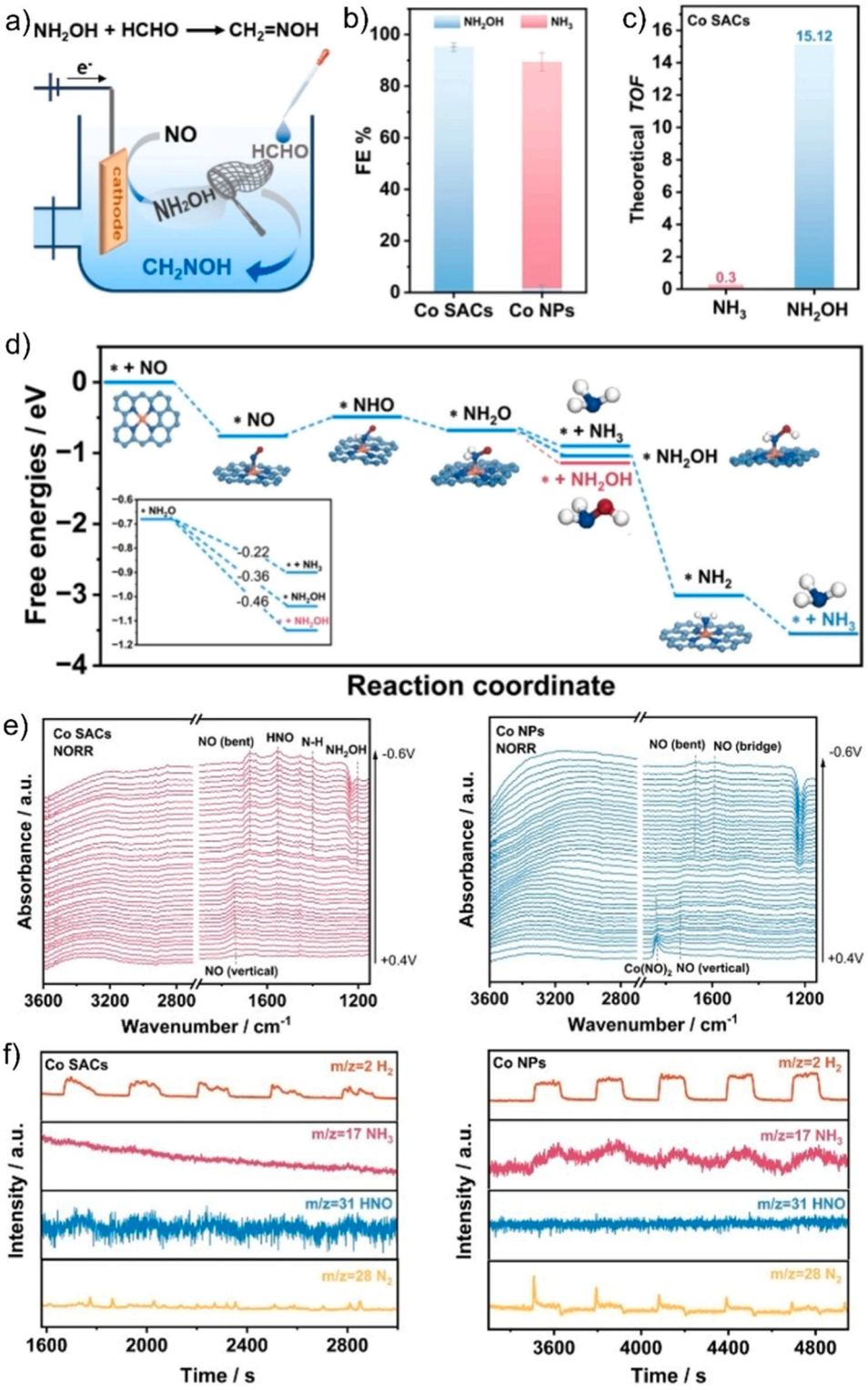

Fig. 2. a) Schematic illustration for in situ capturing NH_2OH with formaldehyde. b) Faradaic efficiency of NH_3 and NH_2OH over Co SACs and Co NPs through an in situ capturing test. c) TOF of NH_3 and NH_2OH over Co SACs obtained by microkinetic modeling. d) Free energy diagram to form NH_2OH and NH_3 over Co SACs. e) Potential-dependent in situ ATR-IR spectra for NORR. (f) Online DEMS measurements in five continuous cycles. Copyright 2023, Wiley-VCH.

significant challenge. The modulation of catalyst electronic structure can change the interaction between the surface and the adsorbed species, changing the intrinsic activity [41]. Therefore, regulating the synthesis process and surface design of catalyst structure were realized for this problem, and the insights into the reaction mechanism was also reviewed. This section discusses the recent catalyst structural regulation methods for improving the NORR active, including the crystal structure, crystal face, coordination structure, single-atom catalyst.

2.2.1. *Crystal structure*

The different crystal phases of nanoparticle could lead to significant difference of surface structure and electronic structure, changing the

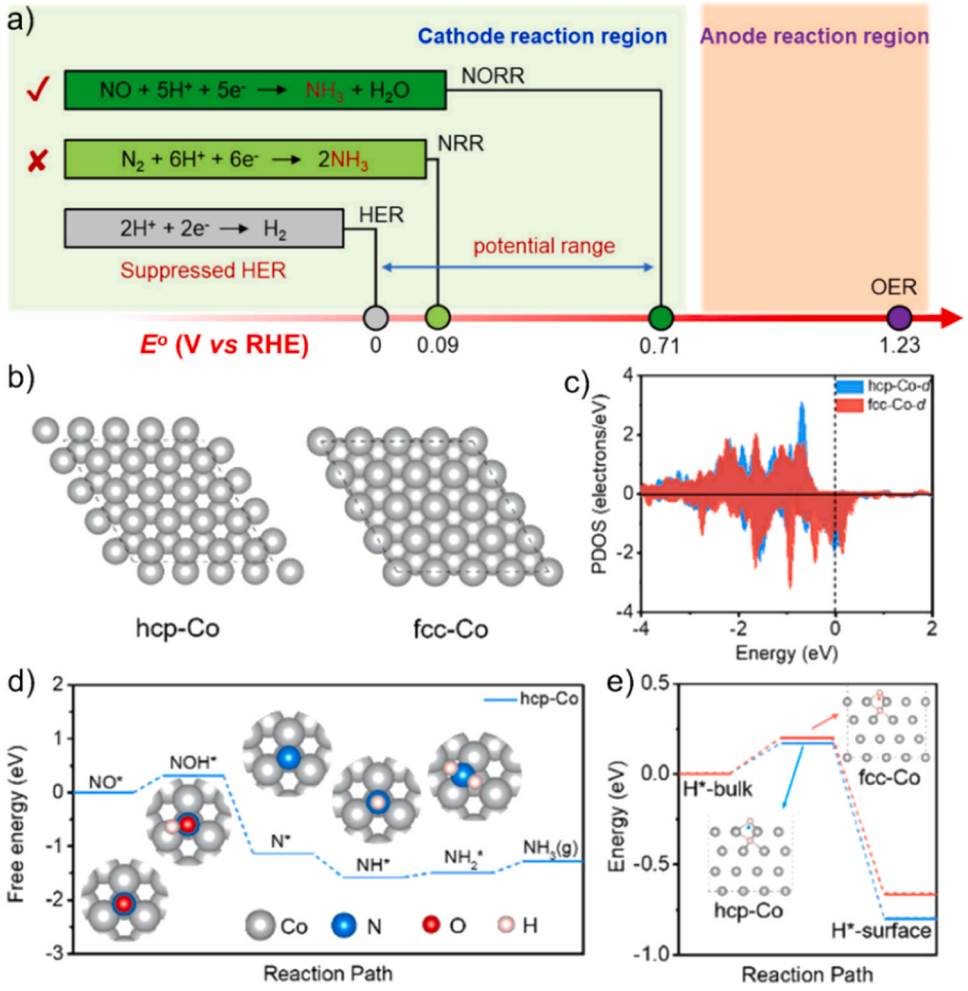

Fig. 3. a) Comparison of standard reduction potentials (E°) for HER, NRR, and NORR. b) Geometrically optimized atomic structure of the hcp-Co and fcc-Co. c) Partial density of states (PDOS) of d orbitals in the hcp-Co and fcc-Co. d) Reaction free energy of NORR. e) Diffusion process of protons from the bulk to the surface of the catalysts. Copyright 2023, American Chemical Society.

activity on the catalyst surface [42]. The geometric structures of the hexagonal-close-packed Co (hcp Co) and the face-centered cubic phase Co (fcc-Co) were prepared and compared, as shown in Fig. 2b. The hcp-Co nanosheet exhibits a high NH_3 yield (439.50 μmol cm^{-2} h^{-1}) and FE (72.58%), which outperform the fcc-Co and the most electrocatalysts reported [43]. The DFT calculations results shows that more up-spin electron-rich features near the Fermi level for the hcp-Co provides a deep electron pool for NORR (Fig. 2c). The NORR activity was enhanced on the hcp-Co due to the unique electron structures and proton shuttle effect. Then, the Zn−NO batteries are assembeld using the hcp-Co as the cathode, showing a power density of 4.66 mW cm^{-2}, superior to the reported catalysts so far. Interestingly, the proton diffusion in hcp-Co exhibits a notably high energetic favorability (ΔG of −0.80 eV), in comparison to that in fcc-Co (ΔG of −0.67 eV), as shown in Fig. 2e. It suggests that there is a greater availability of protons in the hcp-Co for the protonation of NO. The facile proton shuttle effect observed in hcp-Co is of great significance in enhancing the efficiency of electrocatalysis. Similarly, the body-centered cubic RuGa (bcc RuGa) exhibits excellent NORR activity, achieving a remarkable NH_4^+ yield rate (320.6μmol h^{-1} mg^{-1}) and FE (72.3%) [44]. The presence of surrounding gallium (Ga) atoms creates an electron-rich environment around the central ruthenium (Ru) atom. It effectively promotes the adsorption and activation of the *HNO intermediate, leading to a significant reduction in the energy barrier of the potential-determining step (PDS) during NORR process.

Amorphous $B_{2.6}C$ sputtered-deposited on TiO_2 array shows a superb NORR performance for NO- to-NH_3 with a high yield (3678.6 μg h^{-1} cm^{-2}) and FE (87.6%) [45]. Furthermore, it is directly employed as a cathode in a Zn-NO battery, demonstrating a respectable power density (1.7 mW cm^{-2}) and NH_3 yield (1125 μg h^{-1} cm^{-2}). DFT calculations indicate that the B-C bonding could efficiently injects electrons into the NO π2p* orbital, activating NO and facilitating its complete reduction with minimal energy input. This research has the potential to facilitate the development of active and durable catalysts based on amorphous nanoarrays for electrochemical conversion of NO-to-NH_3 applications. Zhu et al. presented an atomically metal clustering catalysts for NORR, and explored the relationship between configuration-activity and the cluster growth. DFT calculation results demonstrated that Co_4 @GaS have a spontaneous thermodynamic barrier of 0.06 eV, such Co_4 cluster is unlimited by convertional volcano-shaped, leading to turning easily electrocatalytic activity [46].

2.2.2. *Crystal face*

Five large-area single-crystal Ni foils with various surface orientations were designed and synthesized to elucidate the structure-function correlation and observed that the high-index Ni facets exhibited higher selectivities toward NH_3 [47]. In particular, Ni(210) achieved 100% selectivity toward NH_3 with a yield rate of 12.02 mmol cm^{-2} h^{-1}. As confirmed by density functional theory (DFT) calculations, the abundant steps on high-index facets facilitated to reduce the energy required for

the hollow-to-bridge location switch of key intermediates associated with the rate-determining hydrogenation step, thereby resulting in a higher NH_3 production capability.

2.2.3. Coordination structure

By stabilizing active atoms through coordination bonds with the substrate, the strong metal-support interactions can be effectively utilized to manipulate the catalytic activity and selectivity for specific reactions. The coordination structure plays a crucial role in influencing the binding energy of reaction intermediates, thereby affecting the catalytic activity [48]. The Ru nanosheets with low coordination numbers (Ru-LCN) exhibit exceptional performance in electrocatalytic reduction of low NO (1% v/v) to NH_3. The faradaic efficiency is measured at 65.96%, with a yield of 45.02 $\mu mol \cdot h^{-1} \cdot mg_{cat}^{-1}$, surpassing its high coordination number counterpart, Ru nanosheets (FE, 37.25%; yield, 25.57 $\mu mol \cdot h^{-1} \cdot mg_{cat}^{-1}$) [49]. Colorimetric methods and ^1H nuclear magnetic resonance spectroscopy are employed for quantitative analysis of NH_3. Fourier transformed infrared microspectroscopy (SR-FTIR) explores and monitors the formation and evolution of chemical bonds during the electrocatalytic process in real time. Through a combination of electrochemical in situ Fourier transform infrared (FT-IR) spectroscopy, online, DEMS, and density functional theory calculations, the researchers unveil the possible reaction pathway and enhanced mechanism. The construction of low coordination number Ru active sites facilitates the adsorption of NO and reduces the energy barrier of the potential-determining hydrogenation step. Moreover, Zhang et al. utilized DFT calculations and a descriptor method to explore systematically catalytic performance of phthalocyanine (MPc) and its derivative with axial chlorine ligand (MPc-Cl) [50]. They proposed a "three-step" strategy, including NO adsorbability, the first hydrogenation step and NH_3 selectivity, to screen the potential NORR candidates. The comparison results demonstrated MPc-Cl with lower limiting potential than MPc, probably because axial Cl ligand coordinated to MPc could increase the NO activation by weakening the bonding strength of NO.

2.2.4. Single-atom catalyst

In recent years, there has been a significant research focus on single atom catalysts, due to their remarkable atomic utilization [51–53]. Catalysts consisting of single metal sites (such as Nb, Al, Mn, Fe, and Cu) supported on nitrogen-doped carbon have shown highly efficient electrocatalytic performance in the NO reduction [54]. However, the maximum FE for NH_3 production on these single metal-site catalysts

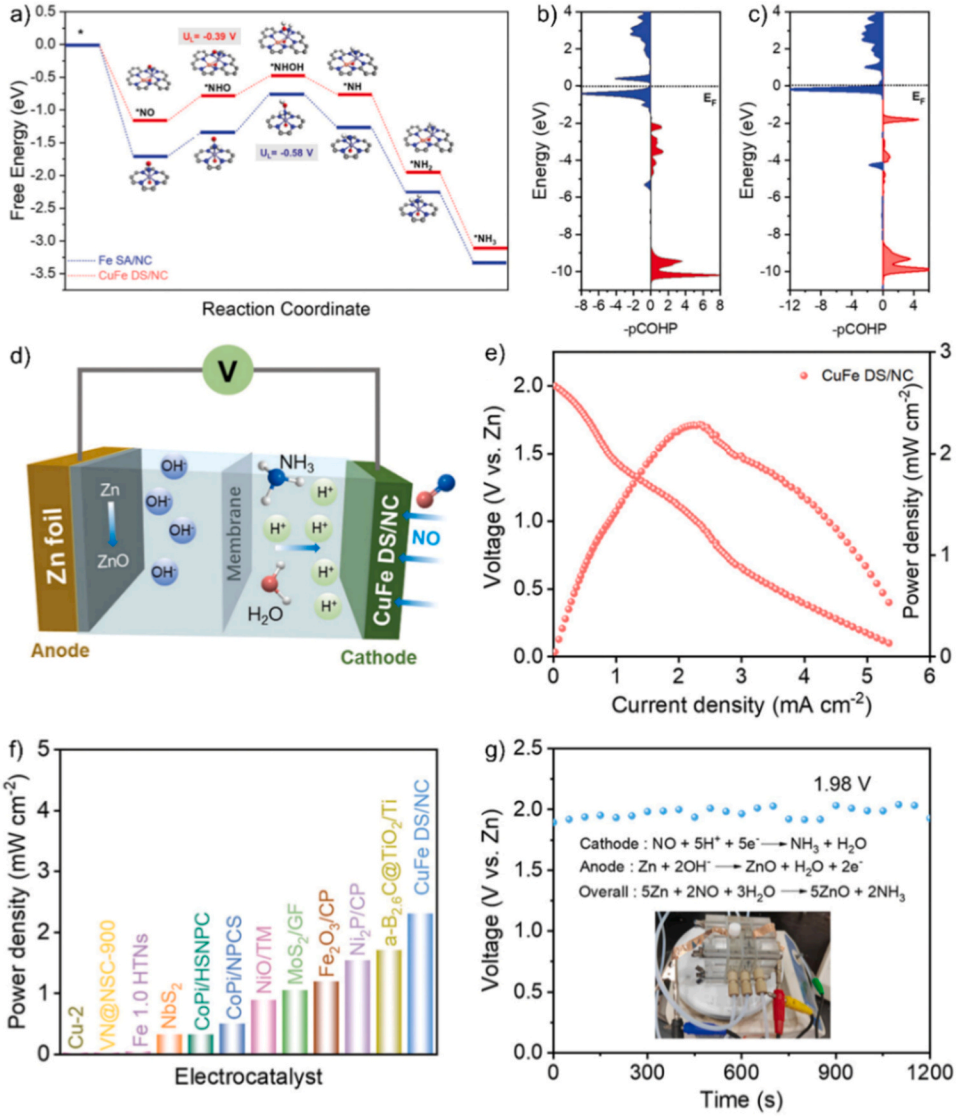

Fig. 4. a) The free energy diagram of NORR. The projected crystal orbital Hamilton population between the metal center of b) Fe SA/NC and c) CuFe DS/NC and the nitrogen atom in NO. d) Schematic diagram of Zn–NO battery. e) Power density and polarization curve. f) Comparison of power density between the metal–NO/N_2 batteries. (g) OCV of the CuFe DS/NC-based Zn–NO battery. Copyright, 2023, American Chemical Society.

remains below 78%. Recent studies have suggested that diatomic site catalysts could greatly enhance electrocatalytic activity by leveraging the synergistic effects of bimetallic sites [55–57]. However, the potential application of diatomic site catalysts in electrocatalytic NO reduction reactions (NORR) has yet to be explored. Therefore, further advancements are required to improve the efficiency of NORR.

Our group reports that an atomic copper-iron dual-site electrocatalyst was utilized on a nitrogen-doped carbon substrate, which is bridged by an axial oxygen atom (O-Fe-N_6-Cu) [58]. This CuFe DS/NC catalyst exhibits a remarkable enhancement in the electrocatalytic synthesis of ammonia by NORR, with a high FE (90%) and yield (112.52 μmol cm^{-2} h^{-1}). These performance metrics are substantially higher compared to previously reported Cu single-atom catalysts, Fe single-atom catalysts, and all other NORR single-atom catalysts. The theoretical calculation results show that the NO reduction follows the *NHO-*NHOH-*NH-*NH_2-NH_3 pathway, and change the rate-determining step from *NHO→*NHOH (Fe SA/NC) to *NO-*NHO (CuFe SA/NC) (Fig. 4a). And meanwhile, the weakened NO-TM interactions in O-CuFe DS/NC accelerates the protonation process to promote electrocatalytic NORR (Fig. 4b, c). Additionally, a proof-of-concept Zn-NO battery (Fig. 4d) was assembled using CuFe DS/NC as the cathode. This battery demonstrated a power density of 2.30 mW cm^{-2} (Fig. 4e), surpassing most previously reported metal--NO/N_2 battery systems (Fig. 4f). Furthermore, it exhibited a high open-circuit voltage (1.98 V) vs. Zn (Fig. 3g), and achieved an NH_3 yield of 45.52 μg h^{-1} mg_{cat}^{-1}. These findings demonstrate the potential of this approach as an efficient and sustainable method for NH_3 synthesis.

The monodispersed iron (Fe) and nickel (Ni) sites with atomically precise coordination environments could promote the NO conversion and regulate the nitrogen-product distribution. FEs and current outputs of three catalysts (SA-M/graphene, M = Fe, Co, and Ni) at various potentials ranging from − 0.14 to − 0.68 V vs. RHE are summarized in Fig. 5a, b. Among these catalysts, Ni exhibits a preference for NH_3 production, achieving a high yield rate (1.6 mmol mg^{-1} h^{-1}). On the

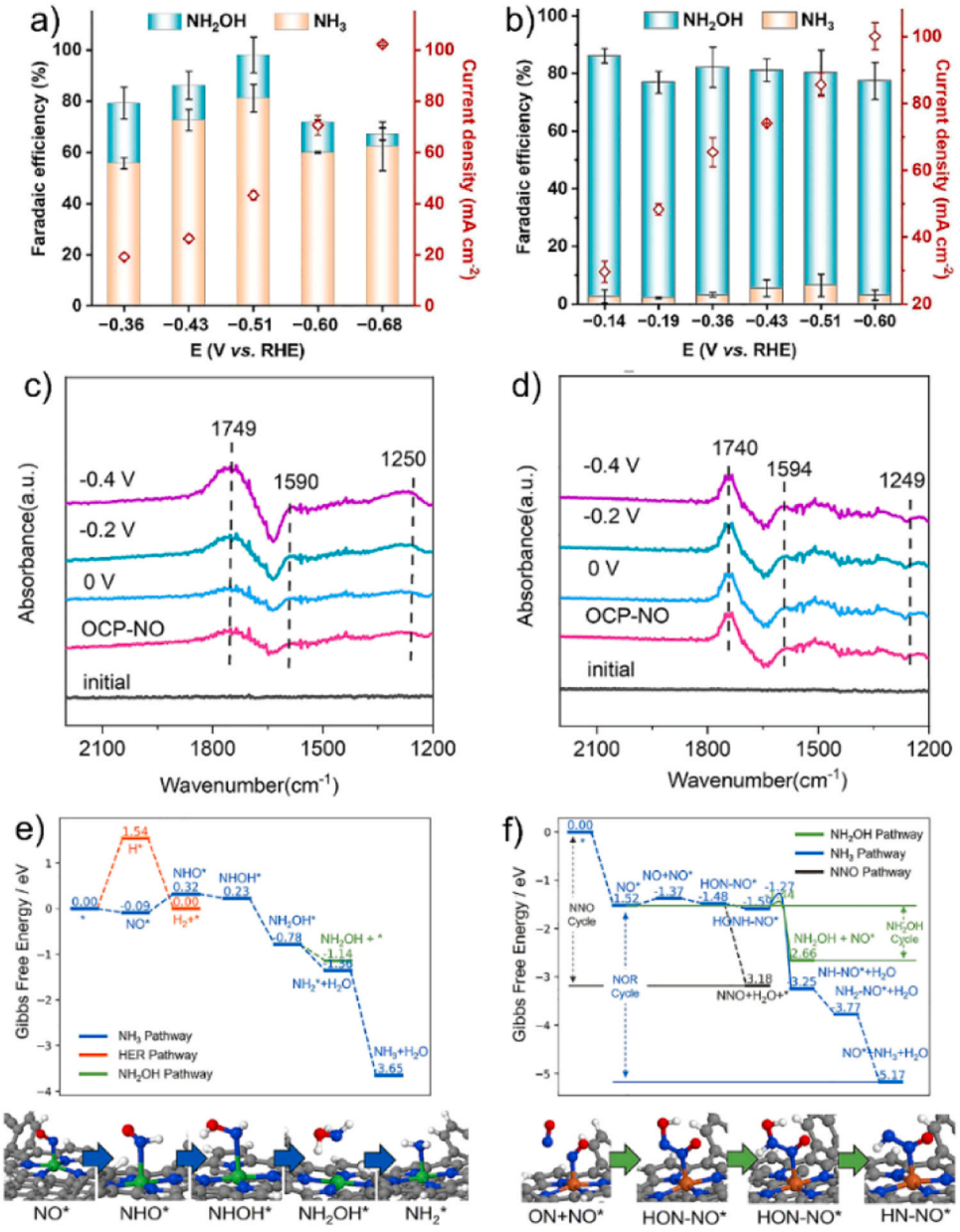

Fig. 5. FEs of NH_3 and NH_2OH and current density on a) SA-Ni/graphene, and b) at different potentials. In situ FT-IR spectra of c) SA-Ni/graphene and d) SA-Fe/graphene. Calculated Gibbs free energy diagrams of reduction pathway. e) SA-Ni/graphene and f) SA-Fe/graphene. Copyright 2022, American Chemical Society.

other hand, Fe demonstrates superior selectivity (83.5%) towards NH_2OH with a record-high production rate of 3.1 mmol mg^{-1} h^{-1}, while Co exhibits relatively lower selectivity [59]. The adsorbate intermediates are studied using operando FT-IR spectroscopy, and distinct peaks are observed on both Ni and Fe surfaces (Fig. 5c, d). The bands at around 1749 and 1740 cm^{-1} correspond to NO* adsorption on Ni and Fe, respectively. The peak intensity on SA-Ni gradually increases at more negative potentials, indicating stronger NO adsorption on Fe, where it can accumulate rapidly. A Gibbs free energy diagram (Fig. 5e) for NO reduction on SA-Ni/graphene reveals that the first proton-coupled electron-transfer step is the potential-determining step (Fig. 5f). The energy barriers indicate that breaking the N-N bond is easier than breaking the N-O bond, suggesting higher selectivity towards NH_2OH.

2.3. The reaction environmental effects

2.3.1. The solution environmental

Under ambient conditions, an electrochemical pathway has been developed to efficiently reduce gaseous NO_x at high reaction rates (400 mA cm^{-2}) [58]. The catalytic role of various transition metals in the electrochemical reduction of NO and N_2O has been investigated to understand their impact on product selectivity. Among them, copper (Cu) exhibits exceptional selectivity towards NH_3 formation, achieving a FE of over 80% in NORR. Additionally, the study on NORR under different partial pressures indicates that a higher NO coverage promotes the N-N coupling reaction. In acidic electrolytes, the formation of NH_3 is significantly favored, while N_2 production is suppressed. To gain further insights into the reaction pathways, mechanistic studies were conducted using flow electrochemical mass spectrometry. Overall, this research offers a promising approach for mitigating gaseous NO_x emissions under ambient conditions with the use of renewable electricity.

2.3.2. The mass transfer regulation

Due to the low NO solubility in solution, the regulation of mass transfer is an efficiency way for improving the NORR active and reaction rate. The metal complex can increase and control the NO solubility, and the most efficient and widely used absorbent is EDTA chelate solution. The ethylene diamine tetraacetic acid (EDTA)–Fe^{2+} metal complex in the electrolyte for rapid NO capture was realized even in a low concentration of NO gas (1%), showing nearly 100% NH_3 FE and ultrahigh stability (more than 120 h) vis nanostructured silver catalyst in NO-to-NH_3 reaction. NO can be absorbed to form a brown product via the Brown-ring reaction by coordinating with Fe^{2+} [60]. The economic benefits of electrochemical NORR NH_3 production was also calculated using phosphate buffered saline (PBS) electrolytes containing EDTA–Fe^{2+}. Constructing gas diffusion electrodes (GDE) is another method to improve NO mass transport [61]. Although enhanced NORR performances can be achieved in the presence of such absorbers for NO capture, industrial-scale applications require simple reaction systems. The GDE with nanoscale zero-valent iron-incorporated of low-concentration NO (1–10%) was developed for the NO to NH_3 reaction, showing a high NH_3 yield (1, 239 μmol·cm^{-2}·h^{-1}) and NH_3 FE (96%). It is more appealing to achieve high NO-to-NH_3 conversion efficiencies in electrolytes with more efficient catalysts.

3. Electrochemical C–N coupling reaction

During the nitric oxide reduction process, the introduction of other carbon species maybe can lead to carbon-nitrogen coupling reactions between the intermediates of carbon species and nitrogen species, resulting in the formation of new products. Recently, our group creatively employed N_2 and CO_2 to realize urea electrosynthesis, which provided a new strategy for C−N coupling for nitrogen fixation [62], which gradually plays an important role which is of great significance for N-cycle. The advent of renewable energy has opened up promising avenues for the electrochemical reduction of NO into higher-value chemicals [63,64]. Considerable endeavors have been dedicated to the production of multi-carbon feedstocks, but there is limited understanding regarding the synthesis mechanisms of nitrogen-containing chemicals. This section will summarize the reactions and mechanisms involving NO, such as C-N coupling with CO_x for urea, and organic molecules for amino acids, oxime, and so on. The different between the two reactions process depends on the different key reactive intermediates, *NO or *NH_2OH from NO, as shown in Fig. 6.

3.1. The C-N coupling mechanisms involving NO

3.1.1. The C-N coupling with CO_x for urea

The reactions process involves two key reactive intermediates, *NO (from NO reduction) and *CO (from CO or CO_2 reduction) for urea. It is a feasible and effective strategy to realize the C−N bond formation for amines generation by co-electrolysis of carbon/nitrogen-containing feedstocks [65]. Deng et al. investigated the production of urea on metal surfaces through the co-reduction of NO and CO [66]. By utilizing DFT calculations to determine the adsorption energies, it is discovered that copper (Cu) has a strong affinity for both *NO and *CO species, but no significant binding with *H. During the co-reduction of NO + CO, two feasible C-N coupling pathways were identified: *CO + *N and *CONH + *N. Further hydrogenation of these intermediates resulted in the formation of urea. To visualize the nitrogen conversion to urea, a 2-D activity heat map was constructed. This study highlights the application of computational simulations in predicting suitable materials with high selectivity and activity for urea production.

It also been then adapted for the preparation of urea by coupling CO_2 and NO [67]. In a flow cell electrolyzer, Zn nanobelts (Zn NBs) demonstrate a urea yield rate of 15.13 mmol h^{-1} g^{-1} and a corresponding FE of 11.26% at 40 mA cm^{-2}. Online DEMS tests reveal the detection of NH_2OH, HNO, NH_3, and CO/N_2 signals when a mixed gas of NO and CO_2 is used as the feed gas (Fig. 7a). Additionally, in situ attenuated total reflection Fourier transform infrared (ATR-FTIR) spectroscopy (Fig. 7b) confirms the formation of C-N bonds through the appearance of a new vibration band at 1465 cm^{-1}. DFT calculations elucidate the electroreduction pathway of NO, which involves the following steps: *NO → *NHO → *NHOH (equivalent to *HNOH) → *NH_2OH → *NH_2 → *NH_3. Simultaneously, *COOH and *CO intermediates facilitate the conversion of CO_2 to CO (Fig. 7c, d). The reaction mechanism for urea synthesis via co-reduction of NO + CO_2 involves a ten-step cascade process, as illustrated in Fig. 7e.

3.1.2. The C-N coupling with organic molecules

The reactions process involves two key reactive intermediates, *NH_2OH (from NO reduction) and *C-species (organic molecules) for the synthesis of amino acids, oxime, and so on.

3.1.2.1. Amino acids. Amino acids have wide application in the food and pharmaceutical industries. Current biotic and chemical syntheses suffer from low efficiency, complex purification operations and high energy consumption. Recently, an innovative method for synthesizing essential α-amino acids from NO was reported through an electrocatalytic process using atomically dispersed Fe supported on an N-doped carbon matrix as the catalyst [68]. The selectivity of the reaction was 11.3%, and a yield of valine with 32.1 μmol mg_{cat}^{-1} was obtained at − 0.6 V vs. RHE. In situ X-ray absorption fine structure and synchrotron radiation infrared spectroscopy analyses revealed that NO was converted to *NH_2OH, which then reacted with the electrophilic carbon center of α-keto acid to form oxime. Subsequent reductive hydrogenation led to the formation of the amino acid, and six kind of different α-amino acids were successfully synthesized as shown in Fig. 9.

Another study by Zhang et al. reported the electrocatalytic synthesis of alanine from NO and pyruvic acid under ambient conditions by oxide-derived Ag with low-coordination sites [69]. Mechanistic studies

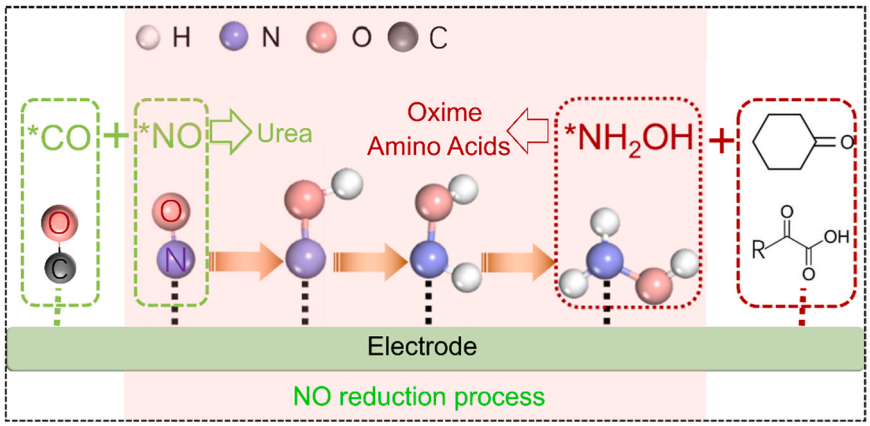

Fig. 6. Schematic of the reactive intermediates during NO reduction process, and the C-N coupling process of *NO with *CO (from CO_2 or CO) for urea, and $*NH_2OH$ (from *NO) with organic molecules for amino acids, oxime, respectively.

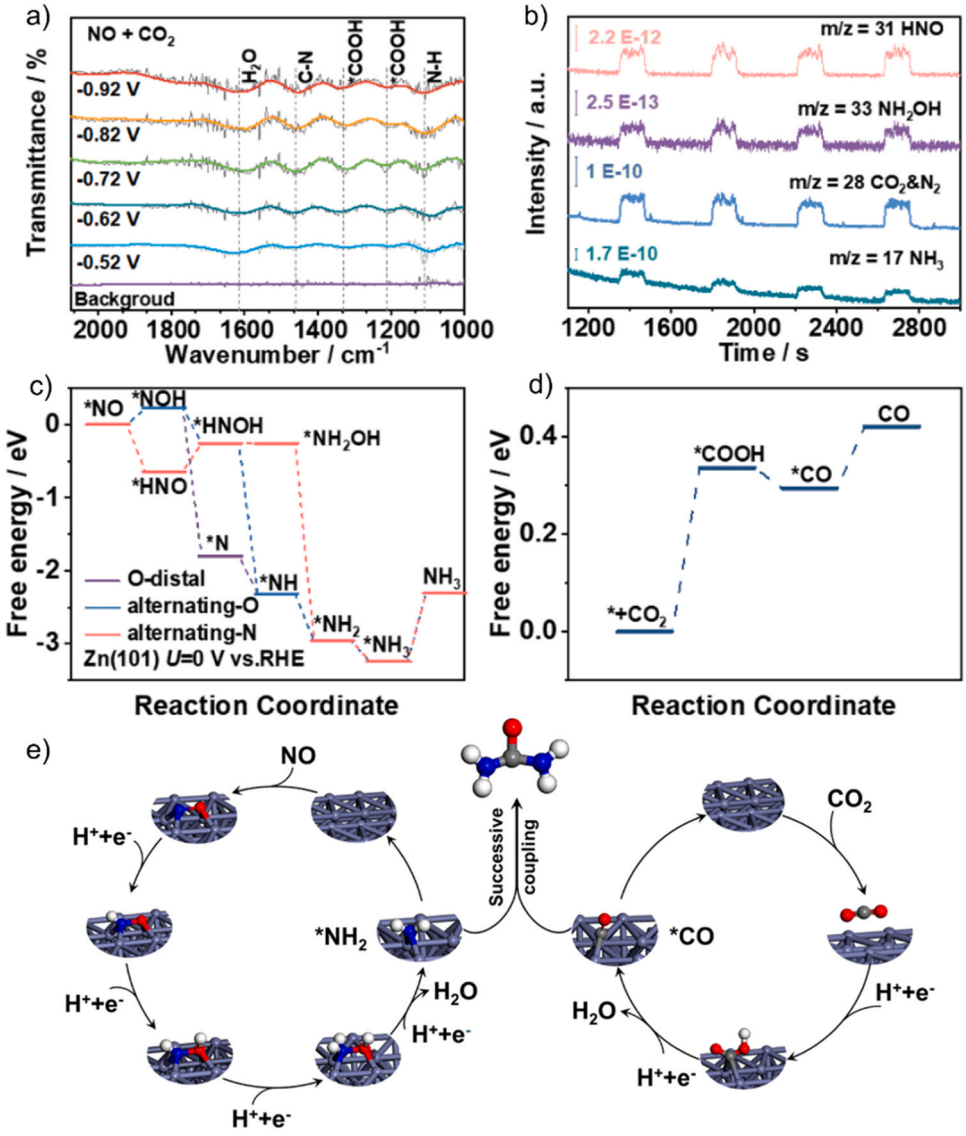

Fig. 7. a) Online DEMS measurements and b) in situ ATR-FTIR spectra over Zn NBs uing NO + CO_2 as the feed gas. Free energy diagram of c) NO and d) CO_2 electroreduction on Zn (101). e) Schematic illustration of urea formation mechanism on the surface of Zn using NO and CO_2 as feed gas. Copyright 2023, American Chemical Society.

showed that the conversion of NO to alanine occurred through a cascade pathway involving *NO → *NH_2OH → *pyruvate oxime → *alanine pathway (Fig. 8d&f). To improve the efficiency of alanine production, a spatially decoupled two-pot electrosynthesis system was designed, which delivered easily purified alanine with a high FE of 70% and a purity of > 98% at 100 mA cm^{-2}. This method not only provides a creative approach to convert nitrogen oxides into valuable products which is of epoch-making significance towards artificial synthesis of amino acids, but also has potential for near-zero-emission technologies.

Very recently, Li et al. proposed the electrosynthesis of amino acid from nitric oxide (NO) and α-keto acids [70]. The reaction mechanisms were demonstrated as the condensation of pyruvic acid (PA) and electrochemically generated *NH_2OH to from pyruvate oxime (PO), and the subsequent electroreduction of PO generates alanine. The electrocatalysts and applied potentials have been optimized, a maximum 17% FE and an 11.45 mmol g^{-1} h^{-1} yield rate of alanine were obtained in the H-type cell. In the two-compartment flow cell, the FE values of PO formation over OD-Ag are all exceed 74% at current densities ranging from 50 to 500 mA cm^{-2}.

3.1.2.2. Oxime. The cyclohexanone oxime (CHO) is a significant C═N organic compound in the industry, serving as the intermediate for Nylon-6 production. However, the traditional method of producing CHO involves a complex and energy-intensive process using expensive NH_3 as

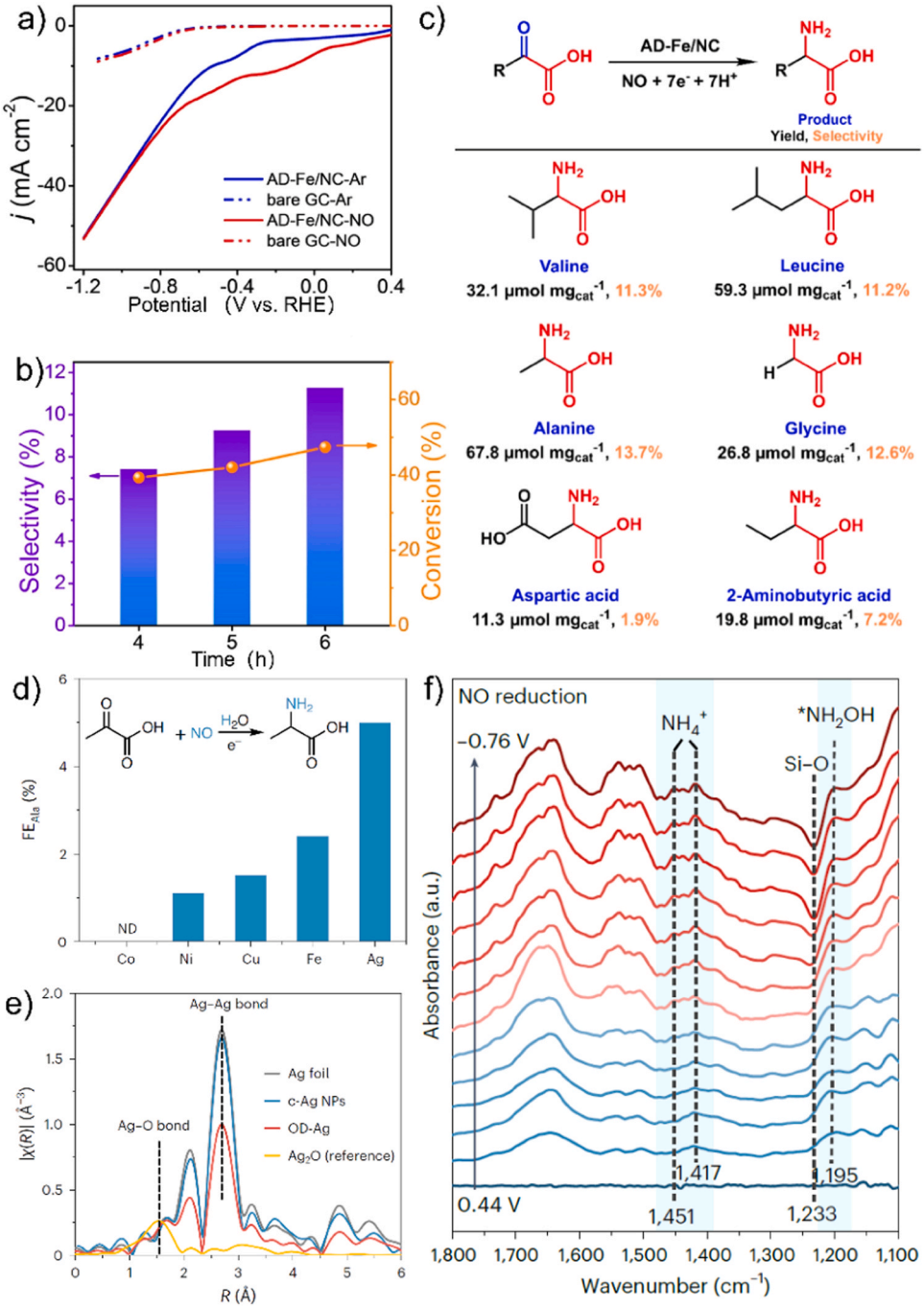

Fig. 8. a) LSV curves of the bare GC and AD-Fe/NC. b) Valine synthesis performance under different conditions. c) Molecular structures of the desired amino acid products and corresponding yield and selectivity. Copyright 2023, Wiley. d) Alanine synthesis over different cathodes. e) EXAFS spectra of OD-Ag and other Ag materials. f) Potential-dependent in situ ATR-FTIR spectra of the electroreduction process. Copyright 2023, Springer Nature.

the nitrogen source and H_2 as the reductant under high temperatures and pressures. The direct one-step synthesis of valuable N-containing organic chemicals from NO remains a big challenging. In a recent study, researchers successfully achieved the direct electrochemical hydrogenative NO for $*NH_2OH$, coupling with cyclohexanone to synthesize CHO (Fig. 9a) [70]. By optimizing the surface hydrophobicity of the catalyst to enhance reactant diffusion, they obtained a high FE of 44.8% and a formation rate of 10.7 mg cm^{-2} h^{-1} for CHO (Fig. 9b). Controlled experiments and ^{15}N-labeling tests confirmed that the nitrogen in the CHO product originated from NO. DFT calculations suggested that the active site for this reaction could be the armchair edge of carbon, following a reaction mechanism of NO → NO* → HNO* → HNOH* → $*NH_2OH$ → CHO. It presents a green electrocatalytic approach for the transformation of NO into valuable C═N organic compounds.

Furthermore, Fe could serve as ideal electrocatalyst for synthesizing CHO from NO_x and cyclohexanone, which could accumulate adsorbed $*NH_2OH$ and cyclohexanone proves to be response for the high efficiency. Similarly, the catalyst (Al-NFM) with Al-O/N unsaturated coordination sites was designed to synthese pyridine oximes by coupling electrochemistry with pyridine aldehydes, and pralidoxime iodide was

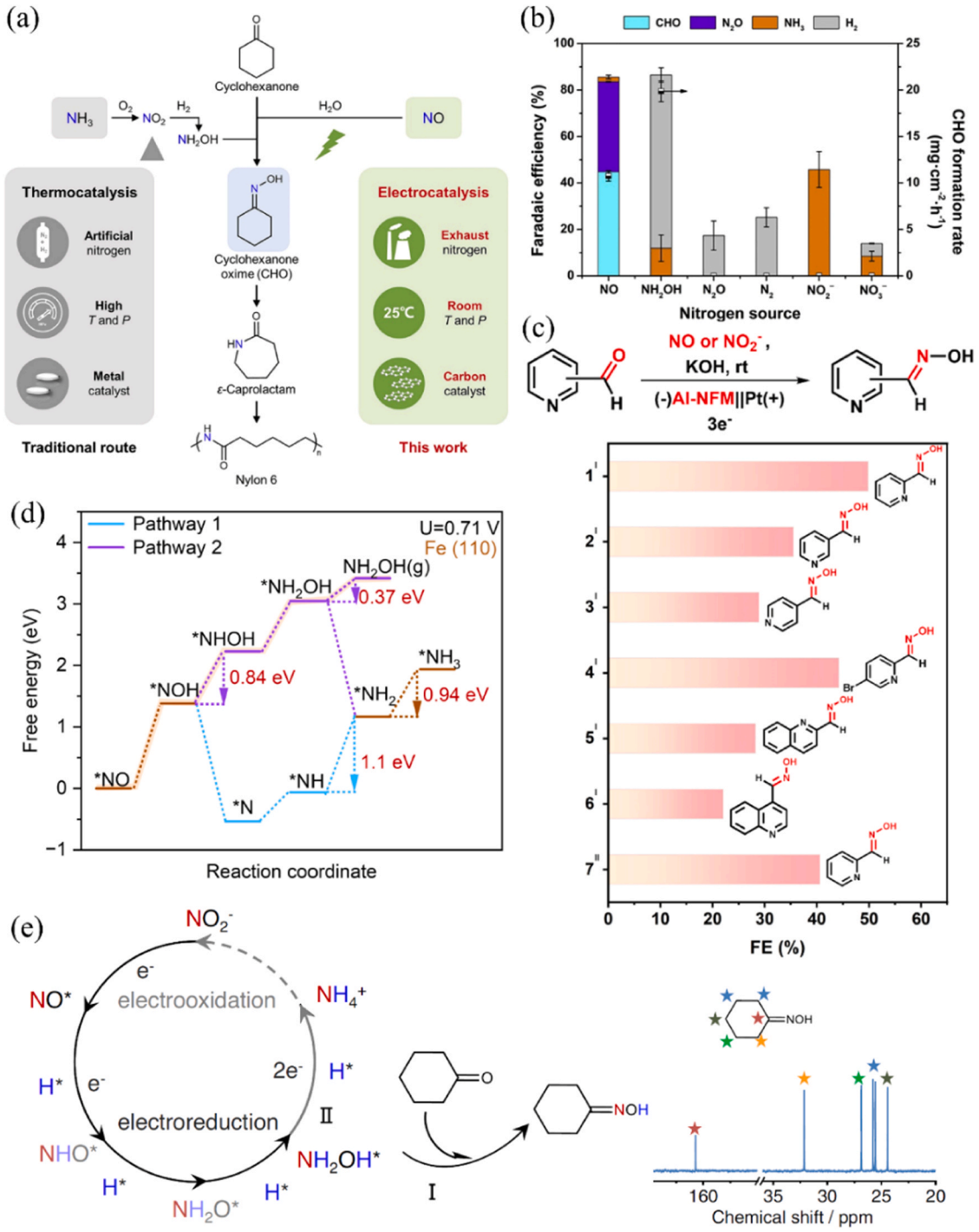

Fig. 9. a) Schematic diagram of the cyclohexanone synthesis from NO. b) FEs and CHO formation rate over different N source. c) The synthetic route for pyridine oximes using in situ generated NH_2OH. d) Free energy profiles NORR pathways on Fe (110). e) Schematic illustration of the cyclohexanone oxime generation pathway, and ^{13}CNMR of cyclohexanone oxime. Copyright 2023, Wiley-VCH.

further synthesized by a simple nucleophilic addition reaction [71]. Through this method, other 5 kinds of pyridine oximes and additional 14 kinds of oximes featuring diverse functional groups, are successful synthesized (Fig. 9**c**). Zhang group developed a Cu-S electrocatalyst to weaken the reduction ability of Cu catalyst with S and stayed at the NH_2OH step. The CuS electrocatalyst was universal for other substrates, such as furfural, cyclopentanone, and cycloheptanone, further broadening the system of electrocatalytic synthesis of oximes (Fig. 9e) [72]. A direct electrosynthesis of cyclohexanone oxime was used nitrogen oxides and cyclohexanone, which eliminated the usage of hydroxylamine

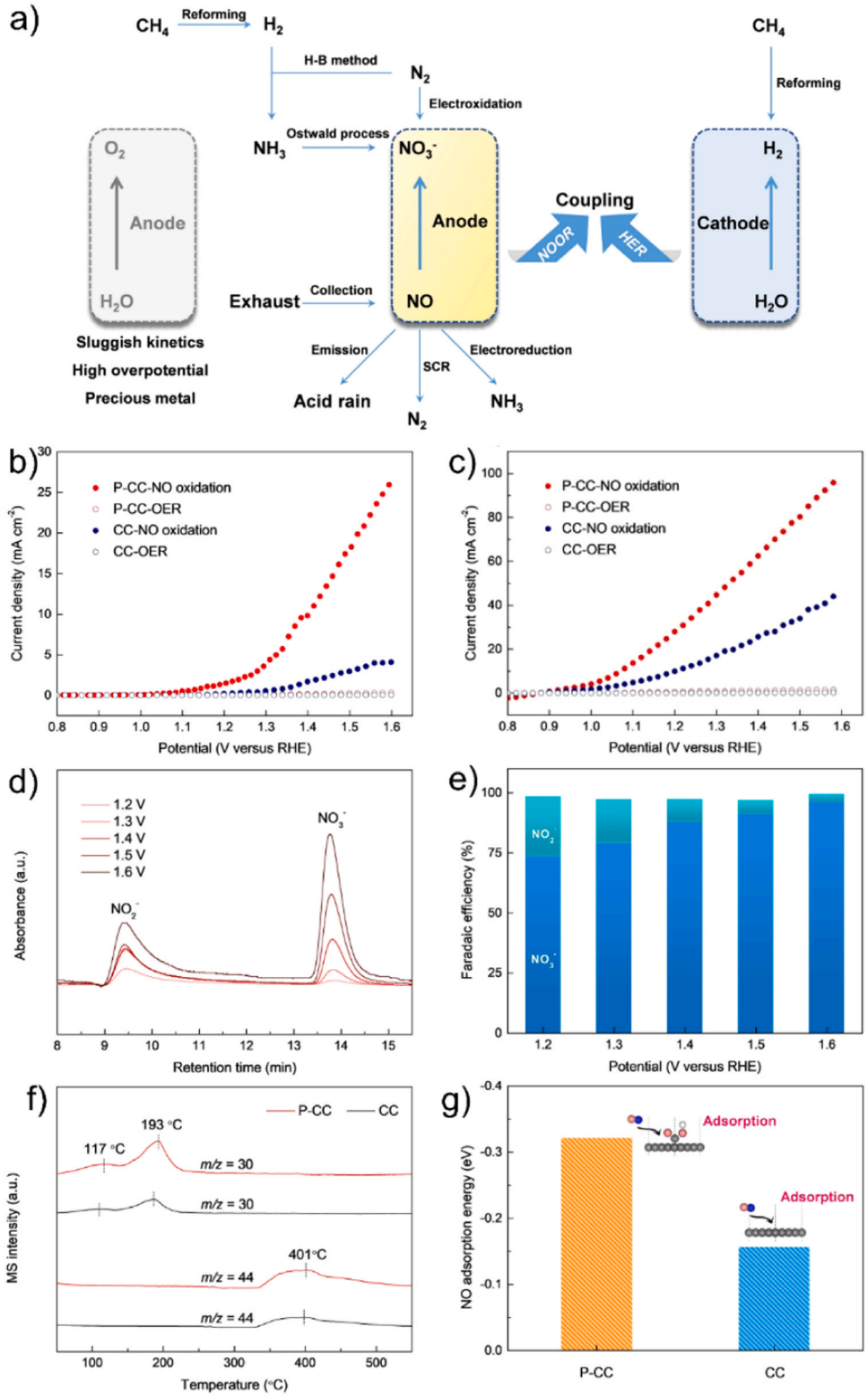

Fig. 10. a) Illustration of the NOR serving as an alternative for the sluggish OER process to achieve sustainable nitrate synthesis at the anode. Electrocatalytic performance of CC and P-CC. b) LSV curves for NO oxidation and OER in 1 M PBS electrolyte. c) LSV curves in 0.5 M H_2SO_4. d) The IC spectra of the nitrite and nitrate products. e) The FEs of nitrite and nitrate at various potentials. f) The NO-TPD spectra. g) The NO adsorption energy. Copyright 2023, Wiley-VCH.

and demonstrated a green production of caprolactam [73]. With the Fe electrocatalysts, a production rate of 55.9 g h^{-1} $gcat^{-1}$ can be achieved in a flow cell with almost 100% yield of cyclohexanone oxime. The high efficiency was attributed to their ability of accumulating adsorbed hydroxylamine and cyclohexanone.

Notable, in the N-cycle reactions (Scheme 1), NO_3^- could be obtained from the oxidation of NO or NH_3, which also could be coupled with CO_2 for the synthesis of urea. The electrocatalytic C-N coupling of CO_2 and nitrate to produce urea offers a promising solution for reducing the environmental impacts of urea production and effectively utilizing waste from various industrial processes [74]. However, the complexity of the electrocatalytic urea synthesis process (involving multiple reactants and reactions) presents challenges for achieving favorable C-N coupling and efficient urea formation. A more sustainable electrocatalytic approach for the direct and selective synthesis of urea from CO_2 and nitrate was reported using an indium hydroxide catalyst [75]. The engineered semiconducting behavior of the catalyst's surface effectively suppressed the HER. The crucial step of C-N coupling began with the reaction between intermediates $*NO_2$ and $*CO_2$. Another study reported the synthesis of urea catalyzed by Cu single atoms supported on CeO_2 [76]. During electrolysis, Cu_4 clusters served as the active sites for urea formation through the reconstitution of Cu single atoms (Cu_1). Additionally, the use of a diatomic catalyst with bonded Fe-Ni pairs demonstrated significant improvements in the efficiency of electrochemical urea synthesis [77]. Compared to isolated diatomic and single-atom catalysts, the bonded Fe-Ni pairs acted as efficient sites for the coordinated adsorption and activation of multiple reactants, enhancing the C-N coupling.

4. The NO oxidation reaction

Nitric acid is of vital importance in various fields such as industrial and agricultural production [78,79]. It is industrially produced through the catalytic oxidation of NH_3 under harsh conditions, which depends on the energy-intensive Haber-Bosch process [80–82]. Recently, room temperature electrochemical nitrogen fixation is considered as a promising new technology that could potentially replace traditional industrial nitrogen fixation methods [83–85]. It has been explored for nitric acid production is N_2 electrooxidation, but with low yield and FE [20,21,86,87,88]. In general, N_2 oxide reduction (NOR) for nitrate salts including two steps [89–91]: (i) the transformation of N_2 into reactive NO* intermediates, which is also the rate-limiting step of NOR. (ii) the NO* intermediate reacts with the O* (generated from electrocatalytic water splitting) to form nitrate salts. For NO, the most common method is selective catalytic reduction (SCR) technology to converts NO into N_2 by consumption of valuable ammonia (NH_3) or hydrogen (H_2). The more promising method for NOOR is to replace the anode reaction.

4.1. The NORR coupling with HER

The more promising method is to convert through electrooxidation, which could also replace the anode OER during water splitting for the green and efficient hydrogen production, especially in neutral and acidic conditions [92,93]. Wang et al. have developed a method that utilizes NO waste through the electrochemical oxidation reaction coupled with HER under ambient conditions [94]. This approach enables efficient H_2 production at the cathode and sustainable nitrate synthesis at the anode simultaneously (Fig. 10a). By this approach, the demand for industrial NH_3 synthesis can be significantly reduced, and the nitrate synthesis pathway can be reformed. The plasma-engraved commercial carbon cloth (P-CC) was utilized as the electrode, which significantly enhanced the NO chemisorption and catalytic activity. Notably, only low potentials of 1.39 V and 1.07 V were needed to achieve a current density of 10 mA cm^{-2} under neutral and acidic conditions, respectively (Fig. 10b, c). The valence state of nitrogen in NO is + 2, the products or NO oxidation are exclusively NO_2^- (+3) and NO_3^- (+5), as shown in Fig. 6d, e. Moreover, NO temperature programmed desorption (NO-TPD) measurements (Fig. 10f) demonstrated that O_2-plasma treatment introduced abundant carboxyl groups into the carbon cloth, enhancing the chemisorption of NO for oxidation activity. DFT calculations further indicated that the introduction of carboxyl groups increased the NO adsorption energy from − 0.157 eV to − 0.322 eV, thereby contributing to enhanced NO adsorption. Additionally, the catalyst exhibited remarkable long-term stability even in highly acidic environments, along with high Faradaic efficiencies approaching 100%.

4.2. The NORR coupling with NOOR

Similarly, Yan et al. reported the electrocatalytic disproportionation of NO, enabling simultaneous synthesis of green NH_3 and nitrate by coupling cathodic NO reduction with anodic NO oxidation [95]. The synergistic effect of CoNi oxide stemmed from the strong active sites of Co-N and optimized adsorption due to electronic structure improvements. Electrochemical NOOR was proposed as an alternative anodic reaction to replace OER, aiming to improve the entire efficiency of the cell. It was observed that acidic conditions favored NOOR with an extremely low onset potential (Fig. 11a).

Moreover, the use of an acid-base decoupled electrolytic environment facilitated by a forward bias bipolar membrane (BPM) played a significant role in enhancing charge-ion transfer and suppressing competitive HER (Fig. 11b). As a result, a remarkable NH_3 production rate of 26.27 mg h^{-1} cm^{-2} with 100% FE was achieved at a low cell voltage of 3.58 V (Fig. 11c). Additionally, the NO utilization efficiency was greatly improved regarding the combination of anodic nitrate production via NO oxidation. The NO oxidation couple with cathode reduction reaction presents an innovative strategy to achieve the resource utilization of NO, sustainable nitrate synthesis, and green and economical H_2 production. However, there are few researches on the NO oxidation reaction at present, showing great research and practical prospect.

5. Conclusion and outlook

Recently, the continuing interest in the electrocatalytic NO reduction (direct NORR and C-N coupling reactions) and oxidation reactions rise gradual for turning this environmentally polluting gas into useful chemicals. In the direct NORR process, the status of the N-O bond (maintenance or breaking) plays a crucial role in regulating product selectivity (NH_2OH or NH_3, respectively). Similarly, the adsorbed state of the NO intermediate also regulated the C-N coupling reactions. The *NO with *CO (from CO or CO_2) for urea, and the $*NH_2OH$ (from the hydrogenation under *NO reduction potential) with organic molecules (α-keto acids or cycloketone) to synthesize amino acid, oxime. With rational catalyst design and optimization of the catalytic system, we focus on the catalyst structure/compositional design, including the defect engineering, crystal plane engineering, atomic engineering, coordination regulation to study the relationship between electronic structure, adsorption energy, and apparent activity sites. The more promising method for NOOR is to replace the anode reaction. However, the design principles of catalysts and the reaction mechanism of most reactions is controversial to be studied further, and there is also faced with many challenges.

(1) The different intermediates indeed play a crucial role in the selectivity of the NORR or the C-N coupling products. For NO to NH_3, the control of the proton concentration within a specific range could improve the NH_3 selectivity. It is worth noting that the researches on the mechanism and application of nitrate reduction reaction to NH_3 has gradually received extensive attention [96–98]. It could provide a new development path and potential, such as water treatment and [99]. During the reaction process, the NO_3^- /NO_2^-/NO are adsorbed and converted to the

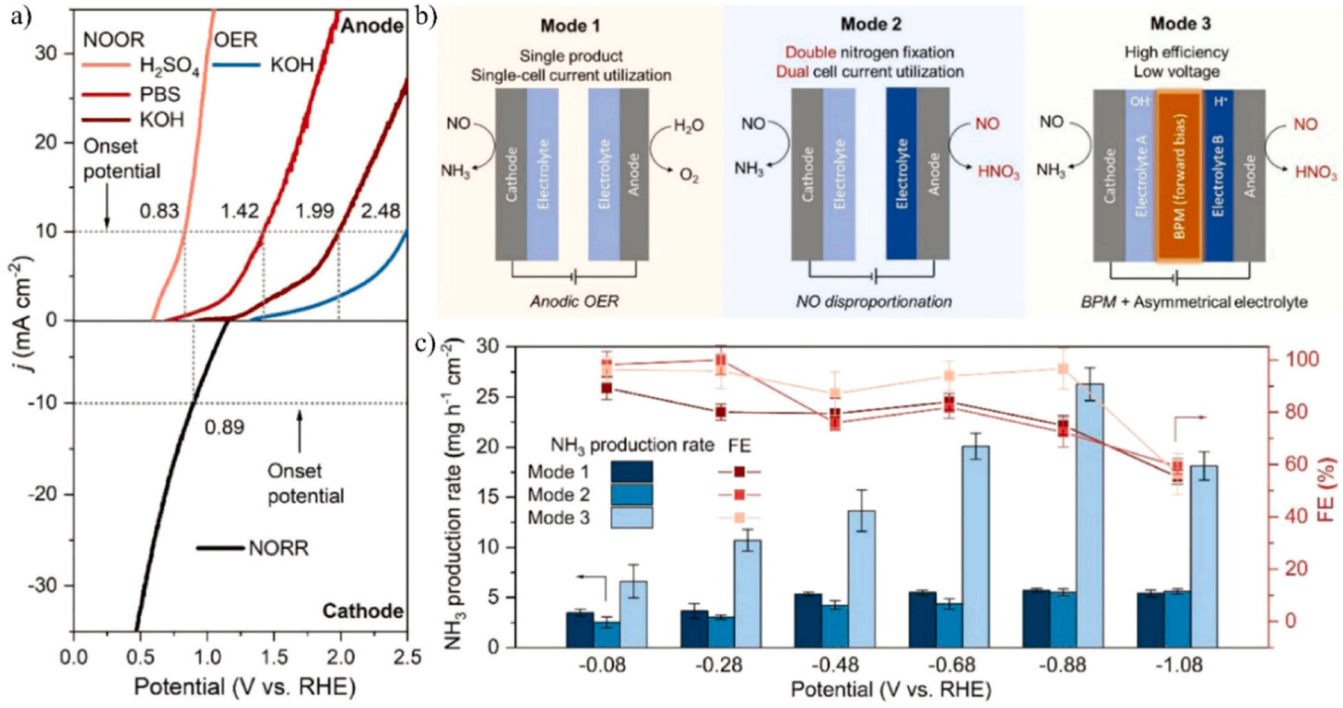

Fig. 11. a) LSV curves of NORR at different conditions. b) Different working modes. Mode 1: NORR with OER; Mode 2: NORR with NOOR; Mode 3: the upgraded NORR/NOOR system with BPM. c) NH_3 production rate and FEs. Copyright 2023, Wiley-VCH.

adsorbed *NO (NO_3^- → *NO_3 → *NO_2 → *NO, NO_2^-→ *NO_2 → *NO; NO→ *NO) [99], which are as the divergent center and control the selectivity for NH_3 or NH_2OH. Noteworthy, how to control N-O bond not to break is the key to selective preparation of NH_2OH, which is also the key intermediate coupling with organic molecules for new productions. It could enrich the range of green synthesis strategy. Designing efficient catalysts to weaken the reduction ability for staying at the NH_2OH step is both importance and challenges. Meanwhile, the reduction reaction on the cathode must enable the formation of carbon anions or carbon radicals as intermediates, which greatly increases the difficulty of catalyst design. The design of catalysts can be achieved by adjusting surface active sites, pore structure, and electron states to selectively adsorb intermediates. For NOOR, it is primarily used as an alternative reaction to OER. However, NO has low solubility in solution, so how to increase its solubility is the key to achieving practical applications. In addition, the main products are nitrate, which is relatively

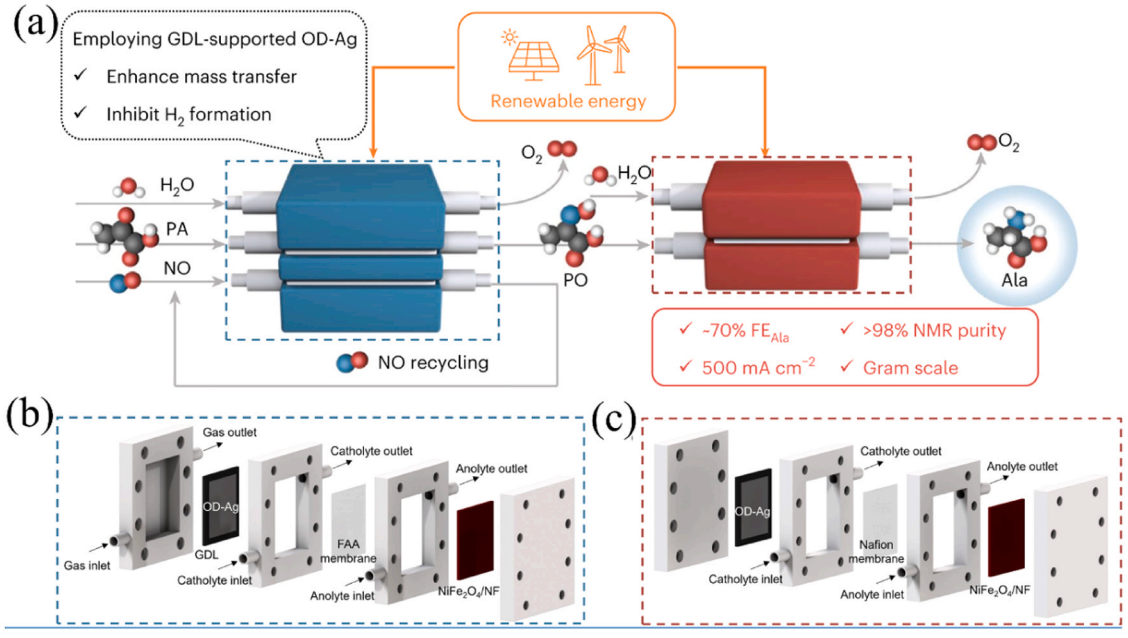

Fig. 12. a) Electrocatalytic C-N coupling to synthesize alanine in electrochemical flow cell. (b) Schematic diagram for the gas-fed three-compartment flow cell for pyruvate oxime (PO) formation from pyruvic acid (PA) and nitric oxide (NO). (c) Schematic diagram for the two-compartment flow cell for PO electroreduction. Copyright 2023, Springer Nature.

homogeneous. Preparing more value-added products from NORR through the catalyst design or new catalytic system become a new trend and challenge. The diversification of reactant species can provide more reaction pathways and possible intermediates, thereby enriching the reaction pathways and product spectrum of electrocatalytic carbon-nitrogen coupling reactions.

(2) The selection of electrochemical reactor configuration is of vital importance for the large-scale chemicals production. Most of reported works rely on the H-type cell with restricted gas diffusion and impeded mass transfer, causing the low current density and undesired product yield. The utilization of flow cell can overcome obstacles of gas diffusion and mass transfer for boosting the scale-up urea synthesis. For example, a spatially decoupled two-pot reaction route has been design, as shown in Fig. 12a. The PA was firstly converted to PO in the gas-fed three-compartment flow cell (Fig. 12b) and the PO reduction to form alanine was achieved in the two-compartment flow cell (Fig. 12c). At current densities ranging and FE of PO formation is markedly improved compared to the H-cell method [68]. It is worth noting that the porosity, hydrophobicity as well as the flow rate of electrolytes deserve to be further optimized. However, the flow cell could suffer from the high ohmic resistance caused by the long distance between cathode and anode. The C-N coupling reactions at carbon and nitrogen simultaneously could reduce the heat production during the device, improving the operating efficiency. However, the reaction mechanism under the operating conditions still needs further investigation.

(3) Further research is required to integrate advanced experimental characterization techniques with theoretical calculations to uncover the catalytic mechanism and facilitate catalyst design. Particularly, the use of advanced in-situ characterization methods is crucial for elucidating the atomic-level structure of catalysts, which can provide insights into the structure-property relationship and the evolution of active sites during the catalytic process, including the adsorption and activation sites for each reactant, the location of the coupling reaction, the mechanism of intermediate interactions, and the driving forces involved. Then, how to change the product selectivity will become the research focus.

CRediT authorship contribution statement

Miao Ruping: Writing – original draft. **Chen Dawei:** Writing – review & editing, Supervision, Resources, Investigation. **Guo Zhiyan:** Supervision, Investigation. **Zhou Yangyang:** Writing – original draft, Supervision, Resources. **Chen Chen:** Writing – review & editing, Validation, Supervision, Resources, Project administration. **Wang Shuangyin:** Supervision, Resources.

Declaration of Competing Interest

The authors declare that they have no known competing financial interests or personal relationships that could have appeared to influence the work reported in this paper.

Data availability

No data was used for the research described in the article.

Acknowledgements

The authors acknowledge support from the National Key R&D Program of China (2020YFA0710000), the National Natural Science Foundation of China (Grant Nos. 21825201, 22102054, 22250006 and 22261160640), Hunan Provincial Science Fund for Distinguished Young Scholars (Grant No. 2023JJ10002), the China Postdoctoral Science Foundation (Grant Nos. BX20200116, 2020M682540, 2023M741117, and 2023M741121), the Science Funds of Jiangxi Province (No. 20224BAB213018).

Appendix A. Supporting information

Supplementary data associated with this article can be found in the online version at doi:10.1016/j.apcatb.2023.123662.

References

[1] N. Lehnert, H.T. Dong, J.B. Harland, A.P. Hunt, C.J. White, Reversing nitrogen fixation, Nat. Rev. Chem. 2 (2018) 278–289.
[2] E. Du, C. Terrer, A.F. Pellegrini, A. Ahlström, C.J. van Lissa, X. Zhao, N. Xia, X. Wu, R.B. Jackson, Global patterns of terrestrial nitrogen and phosphorus limitation, Nat. Geosci. 13 (2020) 221–226.
[3] N. Gruber, J.N. Galloway, An earth-system perspective of the global nitrogen cycle, Nature 451 (2008) 293–296.
[4] E. Vervloessem, M. Aghaei, F. Jardali, N. Hafezkhiabani, A. Bogaerts, Plasma-based N_2 fixation into NO_x: insights from modeling toward optimum yields and energy costs in a gliding arc plasmatron, ACS Sustain. Chem. Eng. 8 (2020) 9711–9720.
[5] Z. Zhang, J.D. Atkinson, B. Jiang, M.J. Rood, Z. Yan, Nitric oxide oxidation catalyzed by microporous activated carbon fiber cloth: an updated reaction mechanism, Appl. Catal. B Environ. 148-149 (2014) 573–581.
[6] P. Granger, V.I. Parvulescu, Catalytic NO_x abatement systems for mobile sources: from three-way to lean burn after-treatment technologies, Chem. Rev. 111 (2011) 3155–3207.
[7] S. Ji, Z. Li, K. Song, H. Li, Y. Li, J. Yang, M. Li, C. Yang, Fabrication of a wide temperature Mn-Ce/TNU-9 catalyst with superior NH_3-SCR activity and strong SO_2 and H_2O tolerance, New J. Chem. 45 (2021) 3857–3865.
[8] J. Chen, P. Fu, D. Lv, Y. Chen, M. Fan, J. Wu, A. Meshram, B. Mu, X. Li, Q. Xia, Unusual positive effect of SO_2 on Mn-Ce mixed-oxide catalyst for the SCR reaction of NO_X with NH_3, Chem. Eng. J. 407 (2021) 127071.
[9] S.-w Liu, R.-t Guo, X. Sun, J. Liu, W.-g Pan, Z.-l Xin, X. Shi, Z.-y Wang, X.-y Liu, H. Qin, The deactivation effect of Cl on V/TiO_2 catalyst for NH_3-SCR process: a DRIFT study, Energy Inst. 92 (2019) 1610–1617.
[10] H. Chen, Y. Xia, R. Fang, H. Huang, Y. Gan, C. Liang, J. Zhang, W. Zhang, X. Liu, The effects of tungsten and hydrothermal aging in promoting NH_3-SCR activity on V_2O_5/WO_3-TiO_2 catalysts, Appl. Surf. Sci. 459 (2018) 639–646.
[11] M. Si, B. Shen, G. Adwek, L. Xiong, L. Liu, P. Yuan, H. Gao, C. Liang, Q. Guo, Review on the NO removal from flue gas by oxidation methods, Environ. Sci. 101 (2021) 49–71.
[12] T. Blejchař, J. Konvička, B. von der Heide, R. Malý, M. Maier, High temperature modification of SNCR technology and its impact on NO_x removal process, EDP Sci. 180 (2018) 02009.
[13] H. Chen, D. Chen, S. Fan, L. Hong, D. Wang, SNCR De-NO_x within a moderate temperature range using urea-spiked hydrazine hydrate as reductant, Chemosphere 161 (2016) 208–218.
[14] J. Zhao, X. Wei, T. Li, S. Li, Effect of HCl and CO on nitrogen oxide formation mechanisms within the temperature window of SNCR, Fuel 267 (2020) 117231.
[15] L. Muzio, G. Quartucy, J. Cichanowiczy, Overview and status of post-combustion NO_x control: SNCR, SCR and hybrid technologies, Int. J. Environ. Pollut. 17 (2002) 4–30.
[16] D. Liu, M. Chen, X. Du, H. Ai, K.H. Lo, S. Wang, S. Chen, G. Xing, X. Wang, H. Pan, Development of electrocatalysts for efficient nitrogen reduction reaction under ambient condition, Adv. Funct. Mater. 31 (2021) 2008983.
[17] Z. Shi, Q. Peng, E. Jiaqiang, B. Xie, J. Wei, R. Yin, G. Fu, Mechanism, performance and modification methods for NH_3-SCR catalysts: a review, Fuel 331 (2023) 125885.
[18] C. Kurien, M. Mittal, Review on the production and utilization of green ammonia as an alternate fuel in dual-fuel compression ignition engines, Energy Convers. Manag. 251 (2022) 114990.
[19] J. Li, S. Lai, D. Chen, R. Wu, N. Kobayashi, L. Deng, H. Huang, A review on combustion characteristics of ammonia as a carbon-free fuel, Front. Energy Res. 9 (2021) 760356.
[20] X. Cui, C. Tang, Q. Zhang, A review of electrocatalytic reduction of dinitrogen to ammonia under ambient conditions, Adv. Energy Mater. 8 (2018) 1800369.
[21] Z. Huang, M. Rafiq, A.R. Woldu, Q.-X. Tong, D. Astruc, L. Hu, Recent progress in electrocatalytic nitrogen reduction to ammonia (NRR), Chem. Rev. 478 (2023) 214981.
[22] M. Zhang, X. Ai, X. Liang, H. Chen, X. Zou, Key role of local chemistry in lattice nitrogen-participated N_2-to-NH_3 electrocatalytic cycle over nitrides, Adv. Funct. Mater. 33 (2023) 2306358.
[23] X. Yan, D. Liu, H. Cao, F. Hou, J. Liang, S.X. Dou, Nitrogen reduction to ammonia on atomic-scale active sites under mild conditions, Small Methods 3 (0219) 1800501.
[24] Y. Yuan, S. Adimi, X. Guo, T. Thomas, Y. Zhu, H. Guo, G.S. Priyanga, P. Yoo, J. Wang, J. Chen, A surface-oxide-rich activation layer (SOAL) on Ni_2MO_3N for a rapid and durable oxygen evolution reaction, Angew. Chem. Int. Ed. 59 (2020) 18036–18041.
[25] C. Roy, B. Sebok, S. Scott, E. Fiordaliso, J. Sørensen, A. Bodin, D. Trimarco, C. Damsgaard, P. Vesborg, O. Hansen, Impact of nanoparticle size and lattice oxygen on water oxidation on $NiFeO_xH_y$, Nat. Catal. 1 (2018) 820–829.

[26] Y. Wang, Y. Zhang, Z. Liu, C. Xie, S. Feng, D. Liu, M. Shao, S. Wang, Layered double hydroxide nanosheets with multiple vacancies obtained by dry exfoliation as highly efficient oxygen evolution electrocatalysts, Angew. Chem. Int. Ed. 56 (2017) 5867–5871.

[27] W. Chen, L. Xu, X. Zhu, Y.C. Huang, W. Zhou, D. Wang, Y. Zhou, S. Du, Q. Li, C. Xie, Unveiling the electrooxidation of urea: intramolecular coupling of the N-N bond, Angew. Chem. Int. Ed. 60 (2021) 7297–7307.

[28] W. Chen, C. Xie, Y. Wang, Y. Zou, C.-L. Dong, Y.-C. Huang, Z. Xiao, Z. Wei, S. Du, C. Chen, Activity origins and design principles of nickel-based catalysts for nucleophile electrooxidation, Chem 6 (2020) 2974–2993.

[29] N. Zhang, Y. Zou, L. Tao, W. Chen, L. Zhou, Z. Liu, B. Zhou, G. Huang, H. Lin, S. Wang, Electrochemical oxidation of 5–hydroxymethylfurfural on nickel nitride/carbon nanosheets: Reaction pathway determined by in situ sum frequency generation vibrational spectroscopy, Angew. Chem. Int. Ed. 131 (2019) 16042–16050.

[30] Z. Hong, Z. Wang, X. Li, Catalytic oxidation of nitric oxide (NO) over different catalysts: an overview, Catal. Sci. Technol. 7 (2017) 3440–3452.

[31] L. Zhang, X. Ji, X. Ren, Y. Ma, X. Shi, Z. Tian, A.M. Asiri, L. Chen, B. Tang, X. Sun, Electrochemical ammonia synthesis via nitrogen reduction reaction on a MoS_2 catalyst: theoretical and experimental studies, Adv. Mater. 30 (2018) 1800191.

[32] H. Wan, Al Bagger, J. Rossmeisl, Electrochemical nitric oxide reduction on metal surfaces, Angew. Chem. Int. Ed. 60 (2021) 21966–21972.

[33] J. Long, C. Guo, X. Fu, H. Jing, G. Qin, H. Li, J. Xiao, Unveiling potential dependence in NO electroreduction to ammonia, J. Phys. Chem. Lett. 12 (2021) 6988–6995.

[34] I. Katsounaros, M.C. Figueiredo, X. Chen, F. Calle-Vallejo, M.T. Koper, Structure- and coverage-sensitive mechanism of NO reduction on platinum electrodes, ACS Catal. 7 (2017) 4660–4667.

[35] C. Tang, L. Chen, H. Li, L. Li, Y. Jiao, Y. Zheng, H. Xu, K. Davey, S.-Z. Qiao, Tailoring acidic oxygen reduction selectivity on single-atom catalysts via modification of first and second coordination spheres, J. Am. Chem. Soc. 143 (2021) 7819–7827.

[36] Y. Xia, X. Zhao, C. Xia, Z.-Y. Wu, P. Zhu, J.Y. Kim, X. Bai, G. Gao, Y. Hu, J. Zhong, Highly active and selective oxygen reduction to H_2O_2 on boron-doped carbon for high production rates, Nat. Commun. 12 (2021) 4225.

[37] Z. Tao, A.J. Pearce, J.M. Mayer, H. Wang, Bridge sites of Au surfaces are active for electrocatalytic CO_2 reduction, J. Am. Chem. Soc. 144 (2022) 8641–8648.

[38] J. Long, S. Chen, Y. Zhang, C. Guo, X. Fu, D. Deng, J. Xiao, Direct electrochemical ammonia synthesis from nitric oxide, Angew. Chem. Int. Ed. 59 (2020) 9711–9718.

[39] H. Niu, Z. Zhang, X. Wang, X. Wan, C. Kuai, Y. Guo, A feasible strategy for identifying single-atom catalysts toward electrochemical NO-to-NH_3 conversion, Small 17 (2021) e2102396.

[40] J. Zhou, S. Han, R. Yang, T. Li, W. Li, Y. Wang, Y. Yu, B. Zhang, Linear adsorption enables NO selective electroreduction to hydroxylamine on single Co sites, Angew. Chem. Int. Ed. 62 (2023) e202305184.

[41] C. Xie, D. Yan, W. Chen, Y. Zou, R. Chen, S. Zang, Y. Wang, X. Yao, S. Wang, Insight into the design of defect electrocatalysts: from electronic structure to adsorption energy, Mater. Today 31 (2019) 47–68.

[42] L. Yang, J. Fan, B. Xiao, W. Zhu, Unveiling “Sabatier principle” for electrocatalytic nitric oxide reduction on single cluster catalysts: a DFT and machine learning guideline, Chem. Eng. J. 468 (2023) 143823.

[43] G.M. Tomboc, X. Zhang, S. Choi, D. Kim, L.Y.S. Lee, K. Lee, Stabilization, characterization, and electrochemical applications of high-entropy oxides: critical assessment of crystal phase–properties relationship, Adv. Funct. Mater. 32 (2022) 2205142.

[44] D. Wang, Z.-W. Chen, K. Gu, C. Chen, Y. Liu, X. Wei, C.V. Singh, S. Wang, Hexagonal cobalt nanosheets for high-performance electrocatalytic NO reduction to NH_3, J. Am. Chem. Soc. 145 (2023) 899–6904.

[45] H. Zhang, Y. Li, C. Cheng, J. Zhou, P. Yin, H. Wu, Z. Liang, J. Zhang, Q. Yun, A.-L. Wang, L. Zhu, B. Zhang, W. Cao, X. Meng, J. Xia, Y. Yu, Q. Lu, Isolated electron-rich ruthenium atoms in intermetallic compounds for boosting electrochemical nitric oxide reduction to ammonia, Angew. Chem. Int. Ed. 62 (2023) e202213351.

[46] J. Liang, P. Liu, Q. Li, T. Li, L. Yue, Y. Luo, Q. Liu, N. Li, B. Tang, A.A. Alshehri, I. Shakir, P.O. Agboola, C. Sun, X. Sun, Amorphous boron carbide on titanium dioxide nanobelt arrays for high-efficiency electrocatalytic NO reduction to NH_3, Angew. Chem. Int. Ed. 61 (2022) e202202087.

[47] S. Zhao, J. Liu, Z. Zhang, C. Zhu, G. Shi, J. Wu, C. Yang, Q. Wang, M. Chang, K. Liu, S. Li, L. Zhang, Deciphering nickel-catalyzed electrochemical ammonia synthesis from nitric oxide, Chem. https://doi.org/10.1016/j.chempr.2023.08.001.

[48] D. Chen, M. Qiao, Y.-R. Lu, H. Li, D. Liu, C.-L. Dong, Y. Li, S. Wang, Preferential cation vacancies in perovskite hydroxide for oxygen evolution reaction, Angew. Chem. Int. Ed. 57 (2018) 8691–8696.

[49] B. Lu, Q. Liu, S. Chen, Electrocatalysis of single-atom sites: impacts of atomic coordination, ACS Catal. 10 (2020) 7584–7618.

[50] Y. Zhang, J. Lin, Z. Cheng, J. Li, J. Zhu, Q. Zhou, W. Li, G. Zhou, Z. Yang, Theoretical screening, regulation, and prediction of transition metal phthalocyanine electrocatalysts for NO reduction into NH_3, J. Phys. Chem. C. 127 (2023) 21097–21105.

[51] W. Guo, Z. Wang, X. Wang, Y. Wu, General design concept for single-atom catalysts toward heterogeneous catalysis, Adv. Mater. 33 (2021) 2004287.

[52] M. Li, H. Wang, W. Luo, P.C. Sherrell, J. Chen, J. Yang, Heterogeneous single-atom catalysts for electrochemical CO_2 reduction reaction, Adv. Mater. 32 (2020) 2001848.

[53] X. Chen, Y. Guo, X. Du, Y. Zeng, J. Chu, C. Gong, J. Huang, C. Fan, X. Wang, J. Xiong, Atomic structure modification for electrochemical nitrogen reduction to ammonia, Adv. Energy Mater. 10 (2020) 1903172.

[54] X. Peng, Y. Mi, H. Bao, Y. Liu, D. Qi, Y. Qiu, L. Zhuo, S. Zhao, J. Sun, X. Tang, Ambient electrosynthesis of ammonia with efficient denitration, Nano Energy 78 (2020) 105321.

[55] J. d Yi, X. Gao, H. Zhou, W. Chen, Y. Wu, Design of Co-Cu diatomic site catalysts for high-efficiency synergistic CO_2 electroreduction at industrial-level current density, Angew. Chem. Int. Ed. 134 (2022) 202212329.

[56] Z. Pei, X.F. Lu, H. Zhang, Y. Li, D. Luan, X.W. Lou, Highly efficient electrocatalytic oxygen evolution over atomically dispersed synergistic Ni/Co dual sites, Angew. Chem. Int. Ed. 134 (2022), 202207537.

[57] W. Zhang, Y. Chao, W. Zhang, J. Zhou, F. Lv, K. Wang, F. Lin, H. Luo, J. Li, M. Tong, Emerging dual-atomic-site catalysts for efficient energy catalysis, Adv. Mater. 33 (2021) 2102576.

[58] D. Wang, X. Zhu, X. Tu, X. Zhang, C. Chen, X. Wei, Y. Li, S. Wang, Oxygen-bridged copper-iron atomic pair as dual-metal active sites for boosting electrocatalytic NO reduction, Adv. Mater. (2023) 2304646.

[59] B.H. Ko, B. Hasa, H. Shin, Y. Zhao, F. Jiao, Electrochemical reduction of gaseous nitrogen oxides on transition metals at ambient conditions, J. Am. Chem. Soc. 144 (2022) 1258–1266.

[60] J. Liang, Q. Liu, A.A. Alshehri, X. Sun, Recent advances in nanostructured heterogeneous catalysts for N-cycle electrocatalysis, Nano Res. Energy 1 (2022) 2790–8119.

[61] S. Cheon, W.J. Kim, D.Y. Kim, Y. Kwon, J.-I. Han, Electro-synthesis of ammonia from dilute nitric oxide on a gas diffusion electrode, ACS Energy Lett. 7 (2022) 958–965.

[62] C. Chen, X. Zhu, X. Wen, Y. Zhou, L. Zhou, H. Li, L. Tao, Q. Li, S. Du, T. Liu, D. Yan, C. Xie, Y. Zou, Y. Wang, R. Chen, J. Huo, Y. Li, J. Cheng, H. Su, X. Zhao, W. Cheng, Q. Liu, H. Lin, J. Luo, J. Chen, M. Dong, K. Cheng, C. Li, S. Wang, Coupling N_2 and CO_2 in H_2O to synthesize urea under ambient conditions, Nat. Chem. 12 (2020) 717–724.

[63] M. Jouny, J.-J. Lv, T. Cheng, B.H. Ko, J.-J. Zhu, W.A. Goddard III, F. Jiao, Formation of carbon–nitrogen bonds in carbon monoxide electrolysis, Nat. Chem. 11 (2019) 846–851.

[64] T. Fukushima, M. Yamauchi, Electrosynthesis of amino acids from biomass-derivable acids on titanium dioxide, Chem. Commun. 55 (2019) 14721–14724.

[65] H. Wan, X. Wang, L. Tan, M. Filippi, P. Strasser, J. Rossmeisl, Electrochemical synthesis of urea: co-reduction of nitric oxide and carbon monoxide, ACS Catal. 13 (2023) 1926–1933.

[66] C. Chen, N. He, S. Wang, Electrocatalytic C–N coupling for urea synthesis, Small Sci. 1 (2021) 2100070.

[67] Y. Huang, R. Yang, C. Wang, N. Meng, Y. Shi, Y. Yu, B. Zhang, Direct electrosynthesis of urea from carbon dioxide and nitric oxide, ACS Energy Lett. 7 (2021) 284–291.

[68] J. Xian, S. Li, H. Su, P. Liao, S. Wang, Y. Zhang, W. Yang, J. Yang, Y. Sun, Y. Jia, Q. Liu, Q. Liu, G. Li, Electrocatalytic synthesis of essential amino acids from nitric oxide using atomically dispersed Fe on N-doped carbon, Angew. Chem. Int. Ed. 62 (2023) e202304007.

[69] X. Zhang, H. Jing, S. Chen, B. Liu, L. Yu, J. Xiao, D. Deng, Direct electro-synthesis of valuable C═N compound from NO, Chem. Catal. 2 (2022) 1807–1818.

[70] M. Li, Y. Wu, B.-H. Zhao, C. Cheng, J. Zhao, C. Liu, B. Zhang, Electrosynthesis of amino acids from NO and α-keto acids using two decoupled flow reactors, Nat. Catal. 6 (2023) 906–915.

[71] R. Xiang, S. Wang, P. Liao, F. Xie, J. Kang, S. Li, J. Xian, L. Guo, G. Li, Electrocatalytic synthesis of pyridine oximes using in situ generated NH_2OH from NO species on nanofiber membranes derived from NH_2-MIL-53(Al), Angew. Chem. Int. Ed. 62 (2023) e202312239.

[72] Y. Wu, J. Zhao, C. Wang, T. Li, B.-H. Zhao, Z. Song, C. Liu, B. Zhang, Electrosynthesis of a nylon-6 precursor from cyclohexanone and nitrite under ambient conditions, Nat. Commun. 14 (2023) 3057.

[73] Y. Wu, W. Chen, Y. Jiang, Y. Xu, B. Zhou, L. Xu, C. Xie, M. Yang, M. Qiu, D. Wang, Q. Liu, Q. Liu, S. Wang, Y. Zou, Electrocatalytic synthesis of nylon-6 precursor at almost 100% yield, Angew. Chem. Int. Ed. 135 (2023) e202305491.

[74] J. Leverett, T. Tran-Phu, J.A. Yuwono, P. Kumar, C. Kim, Q. Zhai, C. Han, J. Qu, J. Cairney, A.N. Simonov, R.K. Hocking, L. Dai, R. Daiyan, R. Amal, Tuning the coordination structure of Cu-N-C single atom catalysts for simultaneous electrochemical reduction of CO_2 and NO_3^- to urea, Adv. Energy Mater. 12 (2022) 2201500.

[75] C. Lv, L. Zhong, H. Liu, Z. Fang, C. Yan, M. Chen, Y. Kong, C. Lee, D. Liu, S. Li, J. Liu, L. Song, G. Chen, Q. Yan, G. Yu, Selective electrocatalytic synthesis of urea with nitrate and carbon dioxide, Nat. Sustain. 4 (2021) 868–876.

[76] X. Wei, Y. Liu, X. Zhu, S. Bo, L. Xiao, C. Chen, T.T.T. Nga, Y. He, M. Qiu, C. Xie, D. Wang, Q. Liu, F. Dong, C.-L. Dong, X.-Z. Fu, S. Wang, Dynamic reconstitution between copper single atoms and clusters for electrocatalytic urea synthesis, Adv. Mater. 35 (2023) 2300020.

[77] X. Wei, Y. Liu, X. Zhu, S. Bo, L. Xiao, C. Chen, T.T.T. Nga, Y. He, M. Qiu, C. Xie, D. Wang, Q. Liu, F. Dong, C.-L. Dong, X.-Z. Fu, S. Wang, Dynamic reconstitution between copper single atoms and clusters for electrocatalytic urea synthesis, Adv. Mater. 35 (2023) 2300020.

[78] J. Lim, C.A. Fernández, S.W. Lee, M.C. Hatzell, Ammonia and nitric acid demands for fertilizer use in 2050, ACS Energy Lett. 6 (2021) 3676–3685.

[79] J. Lim, C.A. Fernández, S.W. Lee, M.C. Hatzell, Ammonia and nitric acid demands for fertilizer use in 2050, ACS Energy Lett. 6 (2021) 3676–3685.

[80] V. Kyriakou, I. Garagounis, A. Vourros, E. Vasileiou, M. Stoukides, An electrochemical Haber-Bosch process, Joule 4 (2020) 142–158.

[81] M. Capdevila-Cortada, Electrifying the Haber–Bosch, Nat. Catal. 2 (2019), 1055-1055.

[82] J. Humphreys, R. Lan, S. Tao, Development and recent progress on ammonia synthesis catalysts for haber–bosch process, Adv. Energy Sustain. Res. 2 (2021) 2000043.
[83] W. Guo, K. Zhang, Z. Liang, R. Zou, Q. Xu, Electrochemical nitrogen fixation and utilization: theories, advanced catalyst materials and system design, Chem. Soc. Rev. 48 (2019) 5658–5716.
[84] L. Li, C. Tang, H. Jin, K. Davey, S.-Z. Qiao, Main-group elements boost electrochemical nitrogen fixation, Chem 7 (2021) 3232–3255.
[85] Z. Chen, C. Liu, L. Sun, T. Wang, Progress of experimental and computational catalyst design for electrochemical nitrogen fixation, ACS Catal. 12 (2022) 8936–8975.
[86] X.W. Lv, C.C. Weng, Z.Y. Yuan, Ambient ammonia electrosynthesis: current status, challenges, and perspectives, ChemSusChem 13 (2020) 3061–3078.
[87] X. Zhao, G. Hu, G.F. Chen, H. Zhang, S. Zhang, H. Wang, Comprehensive understanding of the thriving ambient electrochemical nitrogen reduction reaction, Adv. Mater. 33 (2021) 2007650.
[88] J. Hou, M. Yang, J. Zhang, Recent advances in catalysts, electrolytes and electrode engineering for the nitrogen reduction reaction under ambient conditions, Nanoscale 12 (2020) 6900–6920.
[89] Y. Liu, J. Zhao, J.M. Lee, Conventional and new materials for selective catalytic reduction (SCR) of NO_x, ChemCatChem 10 (2018) 1499–1511.
[90] L. Han, S. Cai, M. Gao, J.-y Hasegawa, P. Wang, J. Zhang, L. Shi, D. Zhang, Selective catalytic reduction of NOx with NH_3 by using novel catalysts: state of the art and future prospects, Chem. Rev. 119 (2019) 10916–10976.
[91] S. Zhao, J. Peng, R. Ge, S. Wu, K. Zeng, H. Huang, K. Yang, Z. Sun, Research progress on selective catalytic reduction (SCR) catalysts for NO_x removal from coal-fired flue gas, Fuel Process. Technol. 236 (2022) 107432.
[92] K. Kan, T. Xia, L. Li, H. Bi, H. Fu, K. Shi, Amidation of single-walled carbon nanotubes by a hydrothermal process for the electrooxidation of nitric oxide, Nanotechnology 20 (2009) 185502.
[93] X. Xu, L. Yang, S. Jiang, Z. Hu, S. Liu, High reaction activity of nitrogen-doped carbon nanotubes toward the electrooxidation of nitric oxide, Chem. Commun. 47 (2011) 7137–7139.
[94] D. Wang, N. He, L. Xiao, F. Dong, W. Chen, Y. Zhou, C. Chen, S. Wang, Coupling electrocatalytic nitric oxide oxidation over carbon cloth with hydrogen evolution reaction for nitrate synthesis, Angew. Chem. Int. Ed. 60 (2021) 24605–24611.
[95] A. Wu, J. Lv, X. Xuan, J. Zhang, A. Cao, M. Wang, X.Y. Wu, Q. Liu, Y. Zhong, W. Sun, Q. Ye, Y. Peng, X. Lin, Z. Qi, S. Zhu, Q. Huang, X. Li, H.B. Wu, J. Yan, Electrocatalytic disproportionation of nitric oxide toward efficient nitrogen fixation, Adv. Energy Mater. 13 (2023) 2204231.
[96] M. Jiang, M. Zhu, M. Wang, Y. He, X. jun Luo, C. Wu, L. Zhang, Z. Jin, Review on electrocatalytic coreduction of carbon dioxide and nitrogenous species for urea synthesis, ACS Nano 17 (2023) 3209–3224.
[97] M. Jiang, J. Su, X. Song, P. Zhang, M. Zhu, L. Qin, Z. Tie, J. Zuo, Z. Jin, Interfacial reduction nucleation of noble metal nanodots on redox-active metal−organic frameworks for high-efficiency electrocatalytic conversion of nitrate to ammonia, Nano Lett. 22 (2022) 2529–2537.
[98] M. Jiang, A. Tao, Y. Hu, L. Wang, K. Zhang, X. Song, W. Yan, Z. Tie, Z. Jin, Crystalline modulation engineering of Ru nanoclusters for boosting ammonia electrosynthesis from dinitrogen or nitrate, ACS Appl. Mater. Interfaces 14 (2022) 17470–17478.
[99] M. Jiang, Q. Zhu, X. Song, Y. Gu, P. Zhang, C. Li, J. Cui, J. Ma, Z. Tie, Z. Jin, Batch-scale synthesis of nanoparticle-agminated three-dimensional porous Cu@Cu_2O microspheres for highly selective electrocatalysis of nitrate to ammonia, Environ. Sci. Technol. 56 (2022) 10299–10307.